

# 3GPP TR 25.996 V9.0.0 (2009-12)

---

*Technical Report*

## **3rd Generation Partnership Project; Technical Specification Group Radio Access Network; Spatial channel model for Multiple Input Multiple Output (MIMO) simulations (Release 9)**



The present document has been developed within the 3<sup>rd</sup> Generation Partnership Project (3GPP<sup>TM</sup>) and may be further elaborated for the purposes of 3GPP.

The present document has not been subject to any approval process by the 3GPP Organizational Partners and shall not be implemented. This Specification is provided for future development work within 3GPP only. The Organizational Partners accept no liability for any use of this Specification. Specifications and reports for implementation of the 3GPP<sup>TM</sup> system should be obtained via the 3GPP Organizational Partners' Publications Offices.

---

---

**Keywords**

UMTS, radio, antenna

---

**3GPP**

---

**Postal address**

---

**3GPP support office address**

650 Route des Lucioles - Sophia Antipolis  
Valbonne - FRANCE  
Tel.: +33 4 92 94 42 00 Fax: +33 4 93 65 47 16

---

**Internet**

<http://www.3gpp.org>

---

**Copyright Notification**

---

No part may be reproduced except as authorized by written permission.  
The copyright and the foregoing restriction extend to reproduction in all media.

© 2009, 3GPP Organizational Partners (ARIB, ATIS, CCSA, ETSI, TTA, TTC).  
All rights reserved.

UMTS™ is a Trade Mark of ETSI registered for the benefit of its members  
3GPP™ is a Trade Mark of ETSI registered for the benefit of its Members and of the 3GPP Organizational Partners  
LTE™ is a Trade Mark of ETSI currently being registered for the benefit of its Members and of the 3GPP Organizational Partners  
GSM® and the GSM logo are registered and owned by the GSM Association

# Contents

|  |           |
|--|-----------|
| Foreword .....   | 4         |
| 1 Scope .....  | 5         |
| 2 References .....   | 5         |
| 3 Definitions, symbols and abbreviations .....   | 6         |
| 3.1 Definitions .....  | 6         |
| 3.2 Symbols .....  | 6         |
| 3.3 Abbreviations .....  | 6         |
| 4 Spatial channel model for calibration purposes .....   | 6         |
| 4.1 Purpose .....  | 6         |
| 4.2 Link level channel model parameter summary .....   | 7         |
| 4.3 Spatial parameters per path .....  | 8         |
| 4.4 BS and MS array topologies .....   | 8         |
| 4.5 Spatial parameters for the BS .....  | 8         |
| 4.5.1 BS antenna pattern .....   | 8         |
| 4.5.2 Per-path BS angle spread (AS) .....  | 10        |
| 4.5.3 Per-path BS angle of departure .....   | 11        |
| 4.5.4 Per-path BS power azimuth spectrum .....   | 11        |
| 4.6 Spatial parameters for the MS .....  | 11        |
| 4.6.1 MS antenna pattern .....   | 11        |
| 4.6.2 Per-path MS angle spread (AS) .....  | 11        |
| 4.6.3 Per-path MS angle of arrival .....   | 11        |
| 4.6.4 Per-path MS power azimuth spectrum .....   | 12        |
| 4.6.5 MS direction of travel .....   | 12        |
| 4.6.6 Per-path Doppler spectrum .....  | 13        |
| 4.7 Generation of channel model .....  | 13        |
| 4.8 Calibration and reference values .....   | 13        |
| 5 Spatial channel model for simulations .....  | 13        |
| 5.1 General definitions, parameters, and assumptions .....                                     | 14        |
| 5.2 Environments .....   | 16        |
| 5.3 Generating user parameters .....   | 18        |
| 5.3.1 Generating user parameters for urban macrocell and suburban macrocell environments ..... | 18        |
| 5.3.2 Generating user parameters for urban microcell environments .....                        | 20        |
| 5.4 Generating channel coefficients .....  | 22        |
| 5.5 Optional system simulation features .....  | 23        |
| 5.5.1 Polarized arrays .....   | 23        |
| 5.5.2 Far scatterer clusters .....   | 25        |
| 5.5.3 Line of sight .....  | 26        |
| 5.5.4 Urban canyon .....   | 27        |
| 5.6 Correlation between channel parameters .....   | 28        |
| 5.7 Modeling intercell interference .....  | 29        |
| 5.8 System Level Calibration .....   | 30        |
| <b>Annex A: Calculation of circular angle spread .....</b>                                     | <b>38</b> |
| <b>Annex B: Change history .....</b>   | <b>40</b> |

---

## Foreword

This Technical Report has been produced by the 3<sup>rd</sup> Generation Partnership Project (3GPP).

The contents of the present document are subject to continuing work within the TSG and may change following formal TSG approval. Should the TSG modify the contents of the present document, it will be re-released by the TSG with an identifying change of release date and an increase in version number as follows:

Version x.y.z

where:

x the first digit:

- 1 presented to TSG for information;
- 2 presented to TSG for approval;
- 3 or greater indicates TSG approved document under change control.

y the second digit is incremented for all changes of substance, i.e. technical enhancements, corrections, updates, etc.

z the third digit is incremented when editorial only changes have been incorporated in the document.

---

# 1 Scope

The present document details the output of the combined 3GPP-3GPP2 spatial channel model (SCM) ad-hoc group (AHG).

The scope of the 3GPP-3GPP2 SCM AHG is to develop and specify parameters and methods associated with the spatial channel modelling that are common to the needs of the 3GPP and 3GPP2 organizations. The scope includes development of specifications for:

## System level evaluation.

Within this category, a list of four focus areas are identified, however the emphasis of the SCM AHG work is on items a and b.

- a) Physical parameters (e.g. power delay profiles, angle spreads, dependencies between parameters)
- b) System evaluation methodology.
- c) Antenna arrangements, reference cases and definition of minimum requirements.
- d) Some framework (air interface) dependent parameters.

## Link level evaluation.

The link level models are defined only for calibration purposes. It is a common view within the group that the link level simulation assumptions will not be used for evaluation and comparison of proposals.

---

# 2 References

The following documents contain provisions which, through reference in this text, constitute provisions of the present document.

- References are either specific (identified by date of publication, edition number, version number, etc.) or non-specific.
- For a specific reference, subsequent revisions do not apply.
- For a non-specific reference, the latest version applies. In the case of a reference to a 3GPP document (including a GSM document), a non-specific reference implicitly refers to the latest version of that document *in the same Release as the present document*.

- [1] H. M. Foster, S. F. Dehghan, R. Steele, J. J. Stefanov, H. K. Strelouhov, Role of Site Shielding in Prediction Models for Urban Radiowave Propagation (Digest No. 1994/231), IEE Colloquium on Microcellular measurements and their prediction, 1994 pp. 2/1-2/6 .
- [2] L. Greenstein, V. Erceg, Y. S. Yeh, M. V. Clark, "A New Path-Gain/Delay-Spread Propagation Model for Digital Cellular Channels," IEEE Transactions on Vehicular Technology, VOL. 46, NO.2, May 1997, pp.477-485.
- [3] L. M. Correia, Wireless Flexible Personalized Communications, COST 259: European Co-operation in Mobile Radio Research, Chichester: John Wiley & Sons, 2001. Sec. 3.2 (M. Steinbauer and A. F. Molisch, "Directional channel models").

## 3 Definitions, symbols and abbreviations

### 3.1 Definitions

For the purposes of the present document, the following terms and definitions apply.

**Path:** Ray

**Path Component:** Sub-ray

### 3.2 Symbols

For the purposes of the present document, the following symbols apply:

|               |  |
|---------------|--|
| $\sigma_{AS}$ | Angle Spread or Azimuth Spread (Note: unless otherwise stated, the calculation of angle spread will be based on the circular method presented in appendix A) |
| $\sigma_{DS}$ | delay spread   |
| $\sigma_{SF}$ | lognormal shadow fading random variable  |
| $\sigma_{SH}$ | log normal shadow fading constant  |
| $\eta(a, b)$  | represents a random normal (Gaussian) distribution with mean $a$ and variance $b$ .  |

### 3.3 Abbreviations

For the purposes of the present document, the following abbreviations apply:

|     |   |
|-----|---|
| AHG | Ad Hoc Group  |
| AoA | Angle of Arrival  |
| AoD | Angle of Departure  |
| AS  | Angle Spread = Azimuth Spread = $\sigma_{AS}$ (Note: unless otherwise stated, the calculation of angle spread will be based on the circular method presented in appendix A) |
| BS  | Base Station = Node-B = BTS   |
| DoT | Direction of Travel   |
| DS  | delay spread = $\sigma_{DS}$  |
| MS  | Mobile Station = UE = Terminal = Subscriber Unit  |
| PAS | Power Azimuth Spectrum  |
| PDP | Power Delay Profile   |
| PL  | Path Loss   |
| SCM | Spatial Channel Model   |
| SF  | lognormal shadow fading random variable = $\sigma_{SF}$   |
| SH  | log normal shadow fading constant = $\sigma_{SH}$   |
| UE  | User Equipment = MS   |

## 4 Spatial channel model for calibration purposes

This clause describes physical parameters for link level modelling for the purpose of calibration.

### 4.1 Purpose

Link level simulations alone will not be used for algorithm comparison because they reflect only one snapshot of the channel behaviour. Furthermore, they do not account for system attributes such as scheduling and HARQ. For these reasons, link level simulations do not allow any conclusions about the typical behaviour of the system. Only system

level simulations can achieve that. Therefore this document targets system level simulations for the final algorithm comparison.

Link level simulations will not be used to compare performance of different algorithms. Rather, they will be used only for calibration, which is the comparison of performance results from different implementations of a given algorithm.

The description is in the context of a downlink system where the BS transmits to a MS; however the material in this

## 4.2 Link level channel model parameter summary

The table below summarizes the physical parameters to be used for link level modelling.

**Table 4.1: Summary SCM link level parameters for calibration purposes**

| Model                           |                   | Case I  |     | Case II   |      | Case III  |      | Case IV     |     |  |
|---------------------------------|-------------------|---|-----|---|------|---|------|-------------|-----|--|
| Corresponding 3GPP Designator*  |                   | Case B  |     | Case C  |      | Case D  |      | Case A      |     |  |
| Corresponding 3GPP2 Designator* |                   | Model A, D, E   |     | Model C   |      | Model B   |      | Model F     |     |  |
| PDP                             |                   | Modified Pedestrian A   |     | Vehicular A   |      | Pedestrian B  |      | Single Path |     |  |
| # of Paths                      |                   | 1) 4+1 (LOS on, K = 6dB)<br>2) 4 (LOS off)  |     | 6   |      | 6   |      | 1           |     |  |
| Relative Path Power (dB)        | Delay (ns)        | 1) 0.0  | 0   | 0,0   | 0    | 0.0   | 0    | 0           | 0   |  |
|                                 |                   | 2) -Inf   |     |   |      |   |      |             |     |  |
|                                 |                   | 1) -6.51  | 0   | -1.0  | 310  | -0.9  | 200  |             |     |  |
|                                 |                   | 2) 0.0  |     |   |      |   |      |             |     |  |
|                                 |                   | 1) -16.21   | 110 | -9.0  | 710  | -4.9  | 800  |             |     |  |
|                                 |                   | 2) -9.7   |     |   |      |   |      |             |     |  |
|                                 |                   | 1) -25.71   | 190 | -10.0   | 1090 | -8.0  | 1200 |             |     |  |
|                                 |                   | 2) -19.2  |     |   |      |   |      |             |     |  |
|                                 |                   | 1) -29.31   | 410 | -15.0   | 1730 | -7.8  | 2300 |             |     |  |
|                                 |                   | 2) -22.8  |     |   |      |   |      |             |     |  |
|                                 |                   |   |     | -20.0   | 2510 | -23.9   | 3700 |             |     |  |
|                                 |                   |   |     |   |      |   |      |             |     |  |
| Speed (km/h)                    |                   | 1) 3<br>2) 30, 120  |     | 3, 30, 120  |      | 3, 30, 120  |      | 3           |     |  |
| UE/Mobile Station               | Topology          | Reference 0.5λ  |     | Reference 0.5λ  |      | Reference 0.5λ  |      | N/A         |     |  |
|                                 | PAS               | 1) LOS on: Fixed AoA for LOS component, remaining power has 360 degree uniform PAS.<br>2) LOS off: PAS with a Laplacian distribution, RMS angle spread of 35 degrees per path |     | RMS angle spread of 35 degrees per path with a Laplacian distribution<br>Or 360 degree uniform PAS. |      | RMS angle spread of 35 degrees per path with a Laplacian distribution |      | N/A         |     |  |
|                                 | DoT (degrees)     | 0   |     | 22.5  |      | -22.5   |      | N/A         |     |  |
|                                 | AoA (degrees)     | 22.5 (LOS component)<br>67.5 (all other paths)  |     | 67.5 (all paths)  |      | 22.5 (odd numbered paths),<br>-67.5 (even numbered paths)             |      | N/A         |     |  |
| Node B/ Base Station            | Topology          | Reference: ULA with 0.5λ-spacing or 4λ-spacing or 10λ-spacing   |     |   |      |   |      |             | N/A |  |
|                                 | PAS               | Laplacian distribution with RMS angle spread of 2 degrees or 5 degrees, per path depending on AoA/AoD   |     |   |      |   |      |             | N/A |  |
|                                 | AoD/AoA (degrees) | 50° for 2° RMS angle spread per path<br>20° for 5° RMS angle spread per path  |     |   |      |   |      |             | N/A |  |
| NOTE:                           |                   | *Designators correspond to channel models previously proposed in 3GPP and 3GPP2 ad-hoc groups.  |     |   |      |   |      |             |     |  |

## 4.3 Spatial parameters per path

Each resolvable path is characterized by its own spatial channel parameters (angle spread, angle of arrival, power azimuth spectrum). All paths are assumed independent. These assumptions apply to both the BS and the MS specific spatial parameters. The above assumptions are in effect only for the Link Level channel model.

## 4.4 BS and MS array topologies

The spatial channel model should allow any type of antenna configuration to be selected, although details of a given configuration must be shared to allow others to reproduce the model and verify the results.

Calibrating simulators at the link level requires a common set of assumptions including a specific set of antenna topologies to define a baseline case. At the MS, the reference element spacing is  $0.5\lambda$ , where  $\lambda$  is the wavelength of the carrier frequency. At the BS, three values for reference element spacing are defined:  $0.5\lambda$ ,  $4\lambda$ , and  $10\lambda$ .

## 4.5 Spatial parameters for the BS

### 4.5.1 BS antenna pattern

The 3-sector antenna pattern used for each sector, Reverse Link and Forward Link, is plotted in Figure 4.1 and is specified by

$$A(\theta) = -\min \left[ 12 \left( \frac{\theta}{\theta_{3dB}} \right)^2, A_m \right] \quad \text{where } -180 \leq \theta \leq 180$$

$\theta$  is defined as the angle between the direction of interest and the boresight of the antenna,  $\theta_{3dB}$  is the 3dB beamwidth in degrees, and  $A_m$  is the maximum attenuation. For a 3 sector scenario  $\theta_{3dB}$  is 70 degrees,  $A_m = 20\text{dB}$ , and the antenna boresight pointing direction is given by Figure 4.2. For a 6 sector scenario  $\theta_{3dB}$  is 35°,  $A_m = 23\text{dB}$ , which results in the pattern shown in Figure 4.3, and the boresight pointing direction defined by Figure 4.4. The boresight is defined to be the direction to which the antenna shows the maximum gain. The gain for the 3-sector 70 degree antenna is 14dBi. By reducing the beamwidth by half to 35 degrees, the corresponding gain will be 3dB higher resulting in 17dBi. The antenna pattern shown is targeted for diversity-oriented implementations (i.e. large inter-element spacings). For beamforming applications that require small spacings, alternative antenna designs may have to be considered leading to a different antenna pattern.



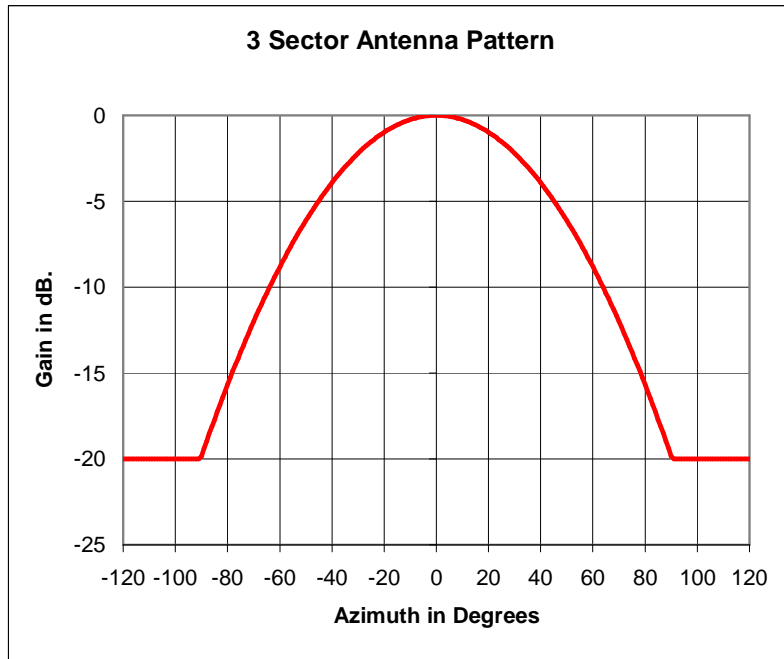


Figure 4.1: Antenna pattern for 3-sector cells

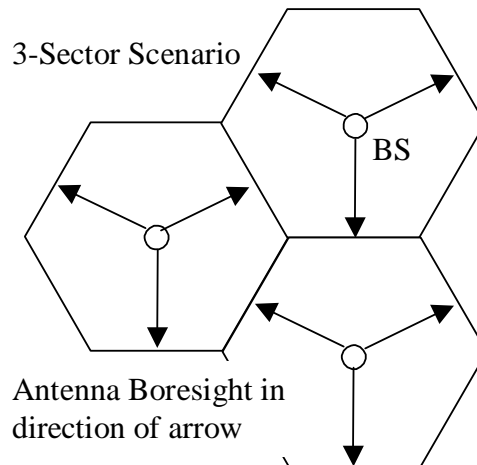
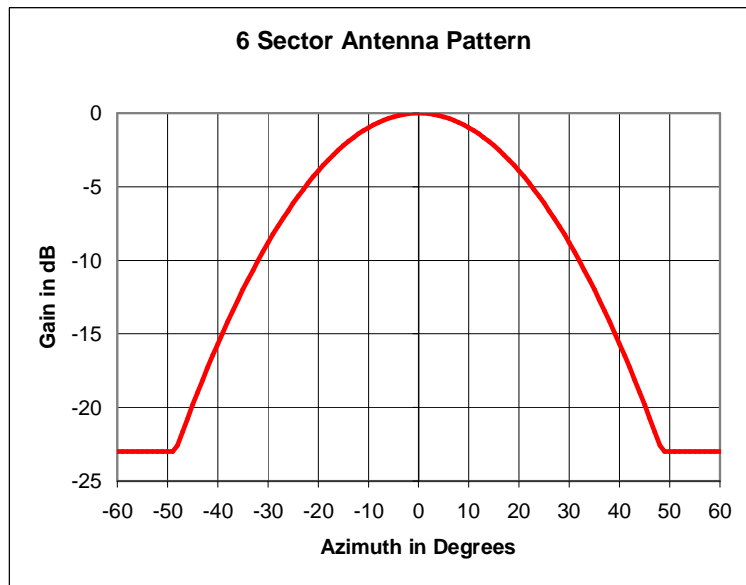
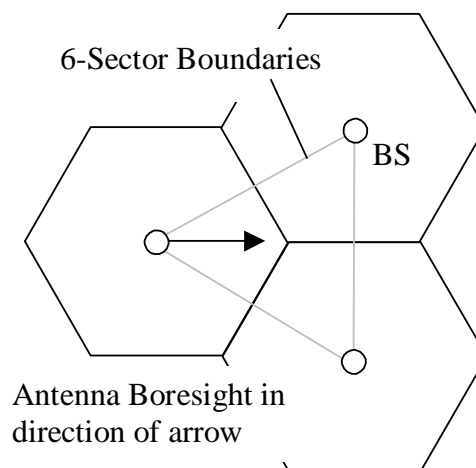


Figure 4.2: Boresight pointing direction for 3-sector cells



**Figure 4.3: Antenna pattern for 6-sector cells**



**Figure 4.4: Boresight pointing direction for 6-sector cells**

#### 4.5.2 Per-path BS angle spread (AS)

The base station per-path angle spread is defined as the root mean square (RMS) of angles with which an arriving path's power is received by the base station array. The individual path powers are defined in the temporal channel model described in Table 4.1. Two values of BS angle spread (each associated with a corresponding mean angle of departure, AoD) are considered:

- AS: 2 degrees at AoD 50 degrees
- AS: 5 degrees at AoD 20 degrees

It should be noted that attention should be paid when comparing the link level performance between the two angle spread values since the BS antenna gain for the two corresponding AoDs will be different. The BS antenna gain is applied to the path powers specified in Table 4.1.

### 4.5.3 Per-path BS angle of departure

The Angle of Departure (AoD) is defined to be the mean angle with which an arriving or departing path's power is received or transmitted by the BS array with respect to the boresite. The two values considered are:

- AoD: 50 degrees (associated with the RMS Angle Spread of 2 degrees)
- AoD: 20 degrees (associated with the RMS Angle Spread of 5 degrees)

### 4.5.4 Per-path BS power azimuth spectrum

The Power Azimuth Spectrum (PAS) of a path arriving at the base station is assumed to have a Laplacian distribution. For an AoD  $\bar{\theta}$  and RMS angle-spread  $\sigma$ , the BS per path PAS value at an angle  $\theta$  is given by:

$$P(\theta, \sigma, \bar{\theta}) = N_o \exp \left[ \frac{-\sqrt{2} |\theta - \bar{\theta}|}{\sigma} \right] G(\theta)$$

where both angles  $\bar{\theta}$  and  $\theta$  are given with respect to the boresight of the antenna elements. It is assumed that all antenna elements' orientations are aligned. Also,  $P$  is the average received power and  $G$  is the numeric base station antenna gain described in Clause 4.5.1 by

$$G(\theta) = 10^{0.1A(\theta)}$$

Finally,  $N_o$  is the normalization constant:

$$N_o^{-1} = \int_{-\pi+\bar{\theta}}^{\pi+\bar{\theta}} \exp \left[ \frac{-\sqrt{2} |\theta - \bar{\theta}|}{\sigma} \right] G(\theta) d\theta$$

In the above equation,  $\theta$  represents path components (sub-rays) of the path power arriving at an AoD  $\bar{\theta}$ .

## 4.6 Spatial parameters for the MS

### 4.6.1 MS antenna pattern

For each and every antenna element at the MS, the antenna pattern will be assumed omni directional with an antenna gain of -1 dBi.

### 4.6.2 Per-path MS angle spread (AS)

The MS per-path AS is defined as the root mean square (RMS) of angles of an incident path's power at the MS array. Two values of the path's angle spread are considered:

- AS: 104 degrees (results from a uniform over 360 degree PAS),
- AS: 35 degrees for a Laplacian PAS with a certain path specific Angle of Arrival (AoA).

### 4.6.3 Per-path MS angle of arrival

The per-path Angle of Arrival (AoA) is defined as the mean of angles of an incident path's power at the UE/Mobile Station array with respect to the broadside as shown Figure 4.5.

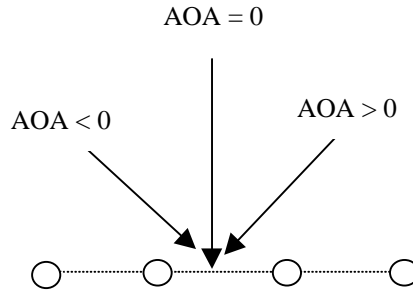


**Figure 4.5: Angle of arrival orientation at the MS.**

Three different per-path AoA values at the MS are suggested for the cases of a non-uniform PAS, see Table 4.1 for details:

- AoA: -67.5 degrees (associated with an RMS Angle Spread of 35 degrees)
- AoA: +67.5 degrees (associated with an RMS Angle Spread of 35 degrees)
- AoA: +22.5 degrees (associated with an RMS Angle Spread of 35 degrees or with an LOS component)

#### 4.6.4 Per-path MS power azimuth spectrum

The Laplacian distribution and the Uniform distribution are used to model the per-path Power Azimuth Spectrum (PAS) at the MS.

The Power Azimuth Spectrum (PAS) of a path arriving at the MS is modeled as either a Laplacian distribution or a uniform over 360 degree distribution. Since an omni directional MS antenna gain is assumed, the received per-path PAS will remain either Laplacian or uniform. For an incoming AoA  $\bar{\theta}$  and RMS angle-spread  $\sigma$ , the MS per-path Laplacian PAS value at an angle  $\theta$  is given by:

$$P(\theta, \sigma, \bar{\theta}) = N_o \exp \left[ \frac{-\sqrt{2}|\theta - \bar{\theta}|}{\sigma} \right],$$

where both angles  $\bar{\theta}$  and  $\theta$  are given with respect to the boresight of the antenna elements. It is assumed that all antenna elements' orientations are aligned. Also, P is the average received power and  $N_o$  is the normalization constant:

$$N_o^{-1} = \int_{-\pi + \bar{\theta}}^{\pi + \bar{\theta}} \exp \left[ \frac{-\sqrt{2}|\theta - \bar{\theta}|}{\sigma} \right] d\theta.$$

In the above equation,  $\theta$  represents path components (sub-rays) of the path power arriving at an incoming AoA  $\bar{\theta}$ . The distribution of these path components is TBD.

#### 4.6.5 MS direction of travel

The mobile station direction of travel is defined with respect to the broadside of the mobile antenna array as shown in Figure 4.6.

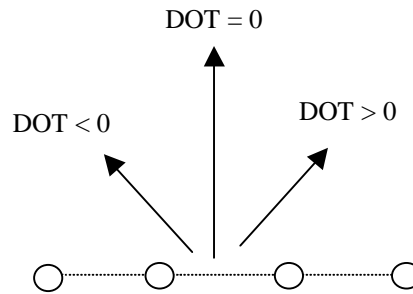


Figure 4.6. Direction of travel for MS

#### 4.6.6 Per-path Doppler spectrum

The per-path Doppler spectrum is defined as a function of the direction of travel and the per-path PAS and AoA at the MS. This should correspond to the per-path fading behavior for either the correlation-based or ray-based method.

### 4.7 Generation of channel model

The proponent can determine the model implementation. Examples of implementations include correlation or ray-based techniques.

### 4.8 Calibration and reference values

For the purpose of link level simulations, reference values of the average correlation are given below in Table 4.2. The reference values are provided for the calibration of the simulation software and to assist in the resolution of possible errors in the simulation methods implemented. Specifically, the average complex correlation and magnitude of the complex correlation is reported between BS antennas and between MS antennas. The spatial parameter values used are those defined already throughout Clause 4.

Table 4.2: Reference correlation values

|    | Antenna Spacing | AS (degrees) | AOA (degrees) | Correlation (magnitude) | Complex Correlation |
|----|-----------------|--------------|---------------|-------------------------|---------------------|
| BS | $0.5\lambda$    | 5            | 20            | 0.9688                  | $0.4743+0.8448i$    |
|    | $0.5\lambda$    | 2            | 50            | 0.9975                  | $-0.7367+0.6725i$   |
|    | $4\lambda$      | 5            | 20            | 0.3224                  | $-0.2144+0.2408i$   |
|    | $4\lambda$      | 2            | 50            | 0.8624                  | $0.8025+0.3158i$    |
|    | $10\lambda$     | 5            | 20            | 0.0704                  | $-0.0617+i0.034$    |
|    | $10\lambda$     | 2            | 50            | 0.5018                  | $-0.2762-i0.4190$   |
| MS | $\lambda/2$     | 104          | 0             | 0.3042                  | -0.3042             |
|    | $\lambda/2$     | 35           | -67.5         | 0.7744                  | $-0.6948-i0.342$    |
|    | $\lambda/2$     | 35           | 22.5          | 0.4399                  | $0.0861+0.431i$     |
|    | $\lambda/2$     | 35           | 67.5          | 0.7744                  | $-0.6948+i0.342$    |

## 5 Spatial channel model for simulations

The spatial channel model for use in the system-level simulations is described in this clause. As in the link level simulations, the description is in the context of a downlink system where the BS transmits to a MS; however the material in this clause (with the exception of Clause 5.7 on loc modelling) can be applied to the uplink as well.

As opposed to link simulations which simply consider a single BS transmitting to a single MS, the system simulations typically consist of multiple cells/sectors, BSs, and MSs. Performance metrics such as throughput and delay are collected over  $D$  drops, where a "drop" is defined as a simulation run for a given number of cells/sectors, BSs, and MSs, over a specified number of frames. During a drop, the channel undergoes fast fading according to the motion of the MSs.

Channel state information is fed back from the MSs to the BSs, and the BSs use schedulers to determine which user(s) to transmit to. Typically, over a series of  $D$  drops, the cell layout and locations of the BSs are fixed, but the locations of the MSs are randomly varied at the beginning of each drop. To simplify the simulation, only a subset of BSs will actually be simulated while the remaining BSs are assumed to transmit with full power. The goal of this clause is to define the methodology and parameters for generating the spatial and temporal channel coefficients between a given base and mobile for use in system level simulations. For an  $S$  element BS array and a  $U$  element MS array, the channel coefficients for one of  $N$  multipath components (note that these components are not necessarily time resolvable, meaning that the time difference between successive paths may be less than a chip period) are given by an  $S$ -by- $U$  matrix of complex amplitudes. We denote the channel matrix for the  $n$ th multipath component ( $n = 1, \dots, N$ ) as  $\mathbf{H}_n(t)$ . It is a function of time  $t$  because the complex amplitudes are undergoing fast fading governed by the movement of the MS. The overall procedure for generating the channel matrices consists of three basic steps:

- 1 Specify an environment, either suburban macro, urban macro, or urban micro (Clause 5.2).
- 2 Obtain the parameters to be used in simulations, associated with that environment (Clause 5.3).
- 3 Generate the channel coefficients based on the parameters (Clause 5.4).

Clauses 5.2, 5.3, and 5.4 give the details for the general procedure. Figure 5.1 below provides a roadmap for generating the channel coefficients. Clause 5.5 specifies optional cases that modify the general procedure. Clause 5.6 describes the procedure for generating correlated log normal user parameters used in Clause 5.3. Clause 5.7 describes the method for accounting for intercell interference. Clause 5.8 presents calibration results.

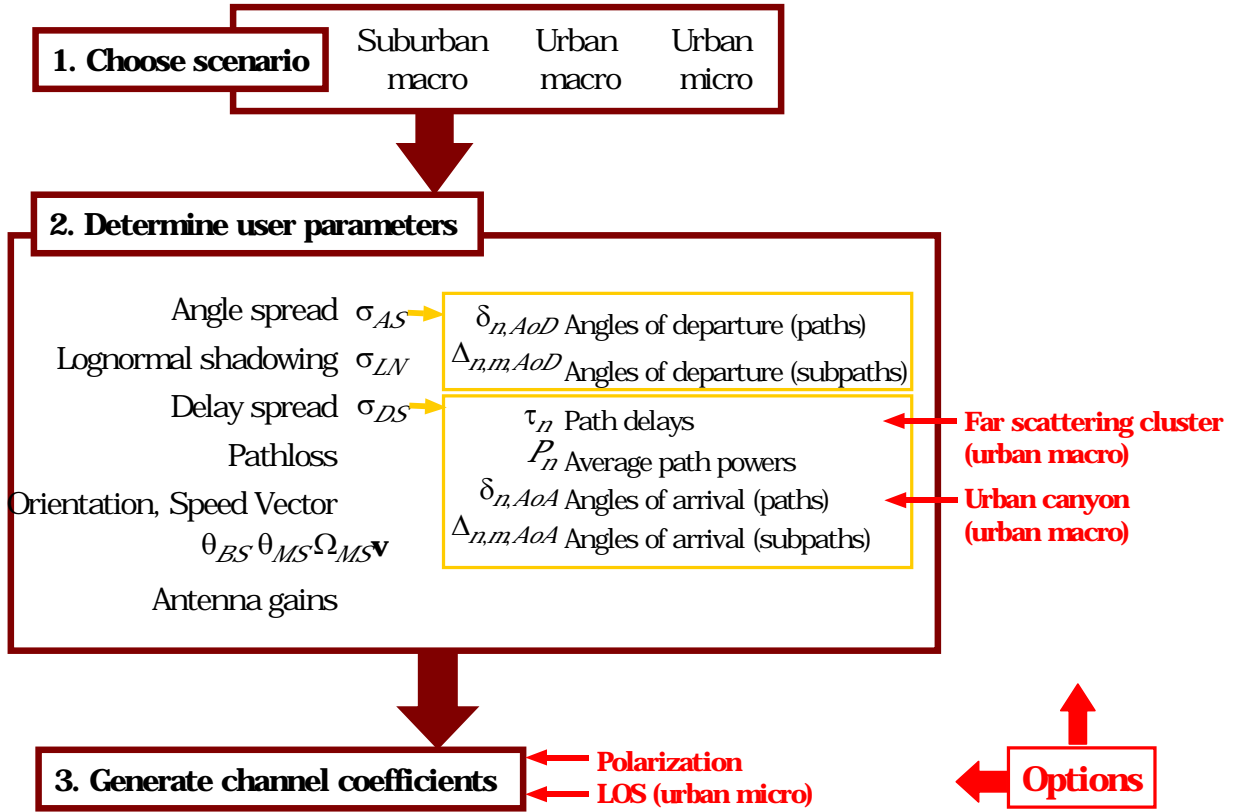


Figure 5.1: Channel model overview for simulations

## 5.1 General definitions, parameters, and assumptions

The received signal at the MS consists of  $N$  time-delayed multipath replicas of the transmitted signal. These  $N$  paths are defined by powers and delays and are chosen randomly according to the channel generation procedure. Each path consists of  $M$  subpaths.

Figure 5.2 shows the angular parameters used in the model. The following definitions are used:

|                    |   |
|--------------------|---|
| $\Omega_{BS}$      | BS antenna array orientation, defined as the difference between the broadside of the BS array and the absolute North (N) reference direction. |
| $\theta_{BS}$      | LOS AoD direction between the BS and MS, with respect to the broadside of the BS array.   |
| $\delta_{n,AoD}$   | AoD for the nth ( $n = 1 \dots N$ ) path with respect to the LOS AoD $\theta_0$ .   |
| $\Delta_{n,m,AoD}$ | Offset for the mth ( $m = 1 \dots M$ ) subpath of the nth path with respect to $\delta_{n,AoD}$ .   |
| $\theta_{n,m,AoD}$ | Absolute AoD for the mth ( $m = 1 \dots M$ ) subpath of the nth path at the BS with respect to the BS broadside.                              |
| $\Omega_{MS}$      | MS antenna array orientation, defined as the difference between the broadside of the MS array and the absolute North reference direction.     |
| $\theta_{MS}$      | Angle between the BS-MS LOS and the MS broadside.   |
| $\delta_{n,AoA}$   | AoA for the nth ( $n = 1 \dots N$ ) path with respect to the LOS AoA $\theta_{0,MS}$ .  |
| $\Delta_{n,m,AoA}$ | Offset for the mth ( $m = 1 \dots M$ ) subpath of the nth path with respect to $\delta_{n,AoA}$ .   |
| $\theta_{n,m,AoA}$ | Absolute AoA for the mth ( $m = 1 \dots M$ ) subpath of the nth path at the MS with respect to the BS broadside.                              |
| $\mathbf{v}$       | MS velocity vector.   |
| $\theta_v$         | Angle of the velocity vector with respect to the MS broadside: $\theta_v = \arg(\mathbf{v})$ .  |

The angles shown in Figure 5.2 that are measured in a clockwise direction are assumed to be negative in value.

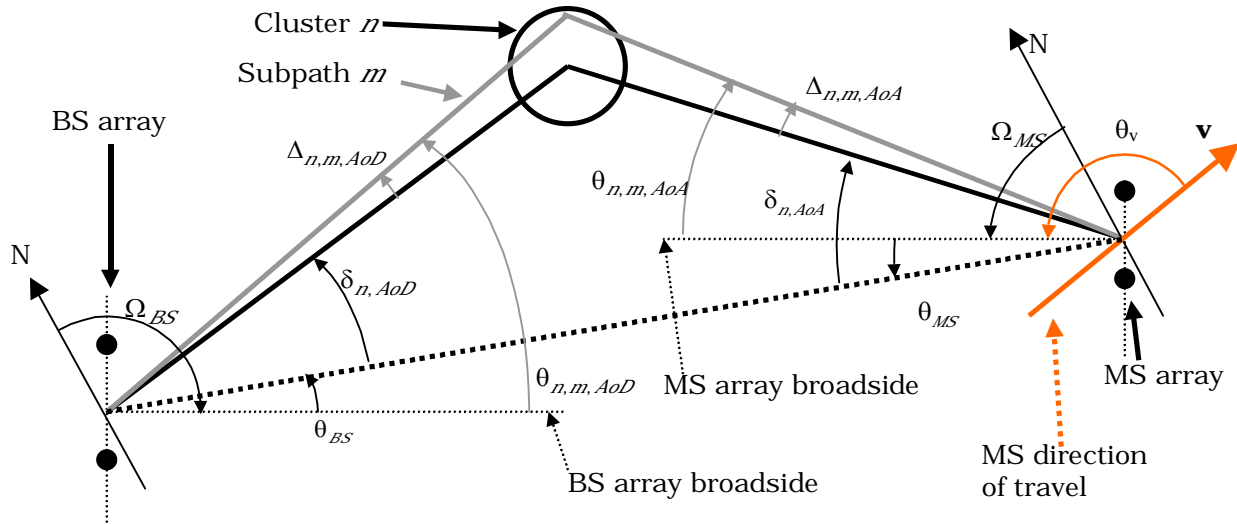


**Figure 5.2: BS and MS angle parameters**

For system level simulation purposes, the fast fading per-path will be evolved in time, although bulk parameters including angle spread, delay spread, log normal shadowing, and MS location will remain fixed during its evaluation during a drop.

The following are general assumptions made for all simulations, independent of environment:

- Uplink-Downlink Reciprocity: The AoD/AoA values are identical between the uplink and downlink.
- For FDD systems, random subpath phases between UL, DL are uncorrelated. (For TDD systems, the phases will be fully correlated.)
- Shadowing among different mobiles is uncorrelated. In practice, this assumption would not hold if mobiles are very close to each other, but we make this assumption just to simplify the model.
- The spatial channel model should allow any type of antenna configuration (e.g. whose size is smaller than the shadowing coherence distance) to be selected, although details of a given configuration must be shared to allow

others to reproduce the model and verify the results. It is intended that the spatial channel model be capable of operating on any given antenna array configuration. In order to compare algorithms, reference antenna configurations based on uniform linear array configurations with 0.5, 4, and 10 wavelength inter-element spacing will be used.

- e) The composite AS, DS, and SF shadow fading, which may be correlated parameters depending on the channel scenario, are applied to all the sectors or antennas of a given base. Sub-path phases are random between sectors. The AS is composed of 6 x 20 sub-paths, and each has a precise angle of departure which corresponds to an antenna gain from each BS antenna. The effect of the antennas gain may cause some change to the channel model in both AS and DS between different base antennas, but this is separate from the channel model. The SF is a bulk parameter and is common among all the BS antennas or sectors.
- f) The elevation spread is not modeled.
- g) To allow comparisons of different antenna scenarios, the transmit power of a single antenna case shall be the same as the total transmit power of a multiple antenna case.
- h) The generation of the channel coefficients (Clause 5.4) assumes linear arrays. The procedure can be generalized for other array configurations, but these modifications are left for the proponent.

## 5.2 Environments

We consider the following three environments.

- a) Suburban macrocell (approximately 3Km distance BS to BS)
- b) Urban macrocell (approximately 3Km distance BS to BS)
- c) Urban microcell (less than 1Km distance BS to BS)

The characteristics of the macro cell environments assume that BS antennas are above rooftop height. For the urban microcell scenario, we assume the BS antenna is at rooftop height. Table 5.1 describes the parameters used in each of the environments.



Table 5.1. Environment parameters

| Channel Scenario  | Suburban Macro   | Urban Macro   | Urban Micro   |
|---|--|---|---|
| Number of paths ( $N$ )   | 6  | 6   | 6   |
| Number of sub-paths ( $M$ ) per-path  | 20   | 20  | 20  |
| Mean AS at BS<br>AS at BS as a lognormal RV<br>$\sigma_{AS} = 10^{\wedge}(\varepsilon_{AS}x + \mu_{AS})$ , $x \sim \eta(0,1)$ | $E(\sigma_{AS})=5^0$<br>$\mu_{AS} = 0.69$<br>$\varepsilon_{AS} = 0.13$ | $E(\sigma_{AS})=8^0, 15^0$<br>$8^0 \mu_{AS} = 0.810$<br>$\varepsilon_{AS} = 0.34$<br>$15^0 \mu_{AS} = 1.18$<br>$\varepsilon_{AS} = 0.210$ | NLOS: $E(\sigma_{AS})=19^0$<br>N/A                              |
| $r_{AS} = \sigma_{AoD} / \sigma_{AS}$   | 1.2  | 1.3   | N/A   |
| Per-path AS at BS (Fixed)   | 2 deg  | 2 deg   | 5 deg (LOS and NLOS)  |
| BS per-path AoD Distribution standard distribution  | $\eta(0, \sigma_{AoD}^2)$ where<br>$\sigma_{AoD} = r_{AS}\sigma_{AS}$  | $\eta(0, \sigma_{AoD}^2)$ where<br>$\sigma_{AoD} = r_{AS}\sigma_{AS}$   | $U(-40\text{deg}, 40\text{deg})$                                |
| Mean AS at MS   | $E(\sigma_{AS, MS})=68^0$  | $E(\sigma_{AS, MS})=68^0$   | $E(\sigma_{AS, MS})=68^0$                                       |
| Per-path AS at MS (fixed)   | $35^0$   | $35^0$  | $35^0$  |
| MS Per-path AoA Distribution  | $\eta(0, \sigma_{AoA}^2(\text{Pr}))$                                   | $\eta(0, \sigma_{AoA}^2(\text{Pr}))$  | $\eta(0, \sigma_{AoA}^2(\text{Pr}))$                            |
| Delay spread as a lognormal RV<br>$\sigma_{DS} = 10^{\wedge}(\varepsilon_{DS}x + \mu_{DS})$ , $x \sim \eta(0,1)$              | $\mu_{DS} = -6.80$<br>$\varepsilon_{DS} = 0.288$                       | $\mu_{DS} = -6.18$<br>$\varepsilon_{DS} = 0.18$   | N/A   |
| Mean total RMS Delay Spread   | $E(\sigma_{DS})=0.17 \mu\text{s}$                                      | $E(\sigma_{DS})=0.65 \mu\text{s}$   | $E(\sigma_{DS})=0.251 \mu\text{s}$ (output)                     |
| $r_{DS} = \sigma_{delays} / \sigma_{DS}$  | 1.4  | 1.7   | N/A   |
| Distribution for path delays  |  |   | $U(0, 1.2\mu\text{s})$  |
| Lognormal shadowing standard deviation, $\sigma_{SF}$   | 8dB  | 8dB   | NLOS: 10dB<br>LOS: 4dB  |
| Pathloss model (dB),<br>$d$ is in meters  | $31.5 + 35\log_{10}(d)$  | $34.5 + 35\log_{10}(d)$   | NLOS: $34.53 + 38\log_{10}(d)$<br>LOS: $30.18 + 26\log_{10}(d)$ |

The following are assumptions made for the *suburban macrocell* and *urban macrocell* environments.

- a) The macrocell pathloss is based on the modified COST231 Hata urban propagation model:

$$PL[dB] = (44.9 - 6.55 \log_{10}(h_{bs})) \log_{10}\left(\frac{d}{1000}\right) + 45.5 + (35.46 - 1.1h_{ms}) \log_{10}(f_c) - 13.82 \log_{10}(h_{bs}) + 0.7h_{ms} + C$$

where  $h_{bs}$  is the BS antenna height in meters,  $h_{ms}$  the MS antenna height in meters,  $f_c$  the carrier frequency in MHz,  $d$  is the distance between the BS and MS in meters, and  $C$  is a constant factor ( $C = 0\text{dB}$  for suburban macro and  $C = 3\text{dB}$  for urban macro). Setting these parameters to  $h_{bs} = 32\text{m}$ ,  $h_{ms} = 1.5\text{m}$ , and  $f_c = 1900\text{MHz}$ , the pathlosses for suburban and urban macro environments become, respectively,  $PL = 31.5 + 35\log_{10}(d)$  and  $PL = 34.5 + 35\log_{10}(d)$ . The distance  $d$  is required to be at least 35m.

- b) Antenna patterns at the BS are the same as those used in the link simulations given in Clause 4.5.1.  
c) Site-to-site SF correlation is  $\zeta = 0.5$ . This parameter is used in Clause 5.6.2.  
d) The hexagonal cell repeats will be the assumed layout.

The following are assumptions made for the *microcell* environment.

- a) The microcell NLOS pathloss is based on the COST 231 Walfish-Ikegami NLOS model with the following parameters: BS antenna height 12.5m, building height 12m, building to building distance 50m, street width 25m, MS antenna height 1.5m, orientation 30deg for all paths, and selection of metropolitan center. With these parameters, the equation simplifies to:

$$PL(dB) = -55.9 + 38 \cdot \log_{10}(d) + (24.5 + 1.5 \cdot f_c/925) \cdot \log_{10}(f_c).$$

The resulting pathloss at 1900 MHz is:  $PL(dB) = 34.53 + 38 \cdot \log_{10}(d)$ , where  $d$  is in meters. The distance  $d$  is at least 20m. A bulk log normal shadowing applying to all sub-paths has a standard deviation of 10dB.

The microcell LOS pathloss is based on the COST 231 Walfish-Ikegami street canyon model with the same parameters as in the NLOS case. The pathloss is

$$PL(dB) = -35.4 + 26 \cdot \log_{10}(d) + 20 \cdot \log_{10}(f_c)$$

The resulting pathloss at 1900 MHz is  $PL(dB) = 30.18 + 26 \cdot \log_{10}(d)$ , where  $d$  is in meters. The distance  $d$  is at least 20m. A bulk log normal shadowing applying to all sub-paths has a standard deviation of 4dB.

- b) Antenna patterns at the BS are the same as those used in the link simulations given in Clause 4.5.1.
- c) Site-to-site correlation is  $\zeta = 0.5$ . This parameter is used in Clause 5.6.2.
- d) The hexagonal cell repeats will be the assumed layout.

Note that the SCM model described here with  $N = 6$  paths may not be suitable for systems with bandwidth higher than 5MHz.

## 5.3 Generating user parameters

For a given scenario and set of parameters given by a column of Table 5.1 Environment parameters, realizations of each user's parameters such as the path delays, powers, and sub-path angles of departure and arrival can be derived using the procedure described here in Clause 5.3. In particular, Clause 5.3.1 gives the steps for the urban macrocell and suburban macrocell environments, and Clause 5.3.2 gives the steps for the urban microcell environments.

### 5.3.1 Generating user parameters for urban macrocell and suburban macrocell environments

**Step 1:** Choose either an urban macrocell or suburban macrocell environment.

**Step 2:** Determine various distance and orientation parameters. The placement of the MS with respect to each BS is to be determined according to the cell layout. From this placement, the distance between the MS and the BS ( $d$ ) and the LOS directions with respect to the BS and MS ( $\theta_{BS}$  and  $\theta_{MS}$ , respectively) can be determined. Calculate the bulk path loss associated with the BS to MS distance. The MS antenna array orientations ( $\Omega_{MS}$ ), are i.i.d., drawn from a uniform 0 to 360 degree distribution. The MS velocity vector  $\mathbf{v}$  has a magnitude  $\|\mathbf{v}\|$  drawn according to a velocity distribution (to be determined) and direction  $\theta_v$  drawn from a uniform 0 to 360 degree distribution.

**Step 3:** Determine the DS, AS, and SF. These variables, given respectively by  $\sigma_{DS}$ ,  $\sigma_{AS}$ , and  $\sigma_{SF}$ , are generated as described in Clause 5.6 below. Note that  $10^{\mu_{DS}}$  is in units of seconds so that the narrowband composite delay spread  $\sigma_{DS}$  is in units of seconds. Note also that we have dropped the BS indices used in Clause 5.6.1 to simplify notation.

**Step 4:** Determine random delays for each of the  $N$  multipath components. For macrocell environments,  $N = 6$  as given in Table 5.1. Generate random variables  $\tau'_1, \dots, \tau'_N$  according to

$$\tau'_n = -r_{DS} \sigma_{DS} \ln z_n \quad n = 1, \dots, N$$

where  $z_n$  ( $n = 1, \dots, N$ ) are i.i.d. random variables with uniform distribution  $U(0,1)$ ,  $r_{DS}$  is given in Table 5.1, and  $\sigma_{DS}$  is derived in Step 3 above. These variables are ordered so that  $\tau'_{(N)} > \tau'_{(N-1)} > \dots > \tau'_{(1)}$  and the minimum of these is subtracted from all. The delay for the  $n$ th path  $\tau_n$  is the value of  $\tau'_{(n)} - \tau'_{(1)}$  are quantized in time to the nearest 1/16th chip interval:

$$\tau_n = \frac{T_c}{16} \cdot \text{floor} \left( \frac{\tau'_{(n)} - \tau'_{(1)}}{T_c/16} + 0.5 \right), \quad n = 1, \dots, N,$$

where floor(x) is the integer part of x, and  $T_c$  is the chip interval ( $T_c = 1/3.84 \times 10^6$  sec for 3GPP and  $T_c = 1/1.2288 \times 10^6$  sec for 3GPP2) Note that these delays are ordered so that  $\tau_N > \tau_5 > \dots > \tau_1 = 0$ . (See notes 1 and 2 at the end of Clause 5.3.1.) Quantization to 1/16 chip is the default value. For special purpose implementations, possibly higher quantization values may be used if needed.

**Step 5:** Determine random average powers for each of the  $N$  multipath components. Let the unnormalized powers be given by

$$P_n = e^{\frac{(1-r_{DS})(\tau'_{(n)} - \tau'_{(1)})}{r_{DS} \sigma_{DS}}} \cdot 10^{-\xi_n/10}, \quad n = 1, \dots, 6$$

where  $\xi_n$  ( $n = 1, \dots, 6$ ) are i.i.d. Gaussian random variables with standard deviation  $\sigma_{RND} = 3$  dB, which is a shadowing randomization effect on the per-path powers. Note that the powers are determined using the unquantized channel delays. Average powers are normalized so that the total average power for all six paths is equal to one:

$$P_n = \frac{P_n}{\sum_{j=1}^6 P_j}.$$

(See note 3 at the end of Clause 5.3.1.)

**Step 6:** Determine AoDs for each of the  $N$  multipath components. First generate i.i.d. zero-mean Gaussian random variables:

$$\delta'_n \sim \eta(0, \sigma_{AoD}^2), \quad n = 1, \dots, N,$$

where  $\sigma_{AoD} = r_{AS} \sigma_{AS}$ . The value  $r_{AS}$  is given in Table 5.1 and depends on whether the urban or suburban macrocell environment is chosen. The angle spread  $\sigma_{AS}$  is generated in Step 3. These variables are given in degrees. They are ordered in increasing absolute value so that  $|\delta'_{(1)}| < |\delta'_{(2)}| < \dots < |\delta'_{(N)}|$ . The AoDs  $\delta_{n,AoD}$ ,  $n = 1, \dots, N$  are assigned to the ordered variables so that  $\delta_{n,AoD} = \delta'_{(n)}$ ,  $n = 1, \dots, N$ . (See note 4 at the end of Clause 5.3.1.)

**Step 7:** Associate the multipath delays with AoDs. The  $n$ th delay  $\tau_n$  generated in Step 3 is associated with the  $n$ th AoD  $\delta_{n,AoD}$  generated in Step 6.

**Step 8:** Determine the powers, phases and offset AoDs of the  $M = 20$  sub-paths for each of the  $N$  paths at the BS. All 20 sub-path associated with the  $n$ th path have identical powers ( $P_n/20$  where  $P_n$  is from Step 5) and i.i.d phases  $\Phi_{n,m}$  drawn from a uniform 0 to 360 degree distribution. The relative offset of the  $m$ th subpath ( $m = 1, \dots, M$ )  $\Delta_{n,m,AoD}$  is a fixed value given in Table 5.2. For example, for the urban and suburban macrocell cases, the offsets for the first and second sub-paths are respectively  $\Delta_{n,1,AoD} = 0.0894$  and  $\Delta_{n,2,AoD} = -0.0894$  degrees. These offsets are chosen to result in the desired per-path angle spread (2 degrees for the macrocell environments, and 5 degrees for the microcell environment). The per-path angle spread of the  $n$ th path ( $n = 1 \dots N$ ) is in contrast to the angle spread  $\sigma_n$  which refers to the composite signal with  $N$  paths.

**Step 9:** Determine the AoAs for each of the multipath components. The AoAs are i.i.d. Gaussian random variables

$$\delta_{n,AoA} \sim \eta(0, \sigma_{n,AoA}^2), \quad n = 1, \dots, N,$$

where  $\sigma_{n,AoA} = 104.12 \left( 1 - \exp(-0.2175 |10 \log_{10}(P_n)|) \right)$  and  $P_n$  is the relative power of the  $n$ th path from Step 5. (See note 5 at the end of Clause 5.3.1)

**Step 10:** Determine the offset AoAs at the UE of the  $M = 20$  sub-paths for each of the  $N$  paths at the MS. As in Step 8 for the AoD offsets, the relative offset of the  $m$ th subpath ( $m = 1, \dots, M$ )  $\Delta_{n,m,AoA}$  is a fixed value given in Table 5.2. These offsets are chosen to result in the desired per-path angle spread of 35 degrees.

**Step 11:** Associate the BS and MS paths and sub-paths. The  $n$ th BS path (defined by its delay  $\tau_n$ , power  $P_n$ , and AoD  $\delta_{n,AoD}$ ) is associated with the  $n$ th MS path (defined by its AoA  $\delta_{n,AoA}$ ). For the  $n$ th path pair, randomly pair each of the  $M$  BS sub-paths (defined by its offset  $\Delta_{n,m,AoD}$ ) with a MS sub-path (defined by its offset  $\Delta_{n,m,AoA}$ ). Each sub-path pair is combined so that the phases defined by  $\Phi_{n,m}$  in step 8 are maintained. To simplify the notation, we renumber the  $M$  MS sub-path offsets with their newly associated BS sub-path. In other words, if the first ( $m = 1$ ) BS sub-path is randomly paired with the 10<sup>th</sup> ( $m = 10$ ) MS sub-path, we re-associate  $\Delta_{n,1,AoA}$  (after pairing) with  $\Delta_{n,10,AoA}$  (before pairing).

**Step 12:** Determine the antenna gains of the BS and MS sub-paths as a function of their respective sub-path AoDs and AoAs. For the  $n$ th path, the AoD of the  $m$ th sub-path (with respect to the BS antenna array broadside) is

$$\theta_{n,m,AoD} = \theta_{BS} + \delta_{n,AoD} + \Delta_{n,m,AoD}.$$

Similarly, the AoA of the  $m$ th sub-path for the  $n$ th path (with respect to the MS antenna array broadside) is

$$\theta_{n,m,AoA} = \theta_{MS} + \delta_{n,AoA} + \Delta_{n,m,AoA}.$$

The antenna gains are dependent on these sub-path AoDs and AoAs. For the BS and MS, these are given respectively as  $G_{BS}(\theta_{n,m,AoD})$  and  $G_{MS}(\theta_{n,m,AoA})$ .

**Step 13:** Apply the path loss based on the BS to MS distance from Step 2, and the log normal shadow fading determined in step 3 as bulk parameters to each of the sub-path powers of the channel model.

#### Notes:

Note 1: In the development of the Spatial Channel Model, care was taken to include the statistical relationships between Angles and Powers, as well as Delays and Powers. This was done using the proportionality factors  $r_{DS} = \sigma_{delays} / \sigma_{DS}$  and  $r_{AS} = \sigma_{AoD} / \sigma_{PAS}$  that were based on measurements.

Note 2: While there is some evidence that delay spread may depend on distance between the transmitter and receiver, the effect is considered to be minor (compared to other dependencies: DS-AS, DS-SF.). Various inputs based on multiple data sets indicate that the trend of DS can be either slightly positive or negative, and may sometimes be relatively flat with distance. For these reasons and also for simplicity, a distance dependence on DS is not modeled.

Note 3: The equations presented here for the power of the  $n$ th path are based on a power-delay envelope which is the average behavior of the power-delay profile. Defining the powers to reproduce the average behavior limits the dynamic range of the result and does not reproduce the expected randomness from trial to trial. The randomizing process  $\xi_n$  is used to vary the powers with respect to the average envelope to reproduce the variations experienced in the actual channel. This parameter is also necessary to produce a dynamic range comparable to measurements.

Note 4: The quantity  $r_{AS}$  describes the distribution of powers in angle and  $r_{AS} = \sigma_{AoD} / \sigma_{PAS}$ , i.e. the spread of angles to the power weighted angle spread. Higher values of  $r_{AS}$  correspond to more power being concentrated in a small AoD or a small number of paths that are closely spaced in angle.

Note 5: Although two different mechanisms are used to select the AoD from the Base, and the AoA at the MS, the paths are sufficiently defined by their BS to MS connection, power  $P_n$ , and delay, thus there is no ambiguity in associating the paths to these parameters at the BS or MS.

### 5.3.2 Generating user parameters for urban microcell environments

Urban microcell environments differ from the macrocell environments in that the individual multipaths are independently shadowed. As in the macrocell case,  $N = 6$  paths are modeled. We list the entire procedure but only describe the details of the steps that differ from the corresponding step of the macrocell procedure.

**Step 1:** Choose the urban microcell environment.

**Step 2:** Determine various distance and orientation parameters.

**Step 3:** Determine the bulk path loss and log normal shadow fading parameters.

**Step 4:** Determine the random delays for each of the  $N$  multipath components. For the microcell environment,  $N = 6$ . The delays  $\tau_n$ ,  $n = 1, \dots, N$  are i.i.d. random variables drawn from a uniform distribution from 0 to 1.2  $\mu\text{s}$ .

**Step 5:** The minimum of these delays is subtracted from all so that the first delay is zero. The delays are quantized in time to the nearest 1/16th chip interval as described in Clause 5.3.1. When the LOS model is used, the delay of the direct component will be set equal to the first arriving path with zero delay.

**Step 6:** Determine random average powers for each of the  $N$  multipath components. The PDP consists of  $N=6$  distinct paths that are uniformly distributed between 0 and 1.2 $\mu\text{s}$ . The powers for each path are exponentially decaying in time with the addition of a lognormal randomness, which is independent of the path delay:

$$P'_n = 10^{-(\tau_n + z_n/10)}$$

where  $\tau_n$  is the unquantized values and given in units of microseconds, and  $z_n$  ( $n = 1, \dots, N$ ) are i.i.d. zero mean Gaussian random variables with a standard deviation of 3dB. Average powers are normalized so that total average power for all six paths is equal to one:

$$P_n = \frac{P'_n}{\sum_{j=1}^6 P'_j}.$$

When the LOS model is used, the normalization of the path powers includes consideration of the power of the direct component  $P_D$  such that the ratio of powers in the direct path to the scattered paths has a ratio of  $K$ :

$$P_n = \frac{P'_n}{(K+1)\sum_{j=1}^6 P'_j}, \quad P_D = \frac{K}{K+1}.$$

**Step 7:** Determine AoDs for each of the  $N$  multipath components. The AoDs (with respect to the LOS direction) are i.i.d. random variables drawn from a uniform distribution over  $-40$  to  $+40$  degrees:

$$\delta_{n,AoD} \sim U(-40, +40), \quad n = 1, \dots, N,$$

Associate the AoD of the  $n$ th path  $\delta_{n,AoD}$  with the power of the  $n$ th path  $P_n$ . Note unlike the macrocell environment, the AoDs do not need to be sorted before being assigned to a path power. When the LOS model is used, the AoD for the direct component is set equal to the line-of-sight path direction.

**Step 8:** Randomly associate the multipath delays with AoDs.

**Step 9:** Determine the powers, phases, and offset AoDs of the  $M = 20$  sub-paths for each of the  $N$  paths at the BS. The offsets are given in Table 5.2, and the resulting per-path AS is 5 degrees instead of 2 degrees for the macrocell case. The direct component, used with the LOS model will have no per-path AS.

**Step 10:** Determine the AoAs for each of the multipath components. The AoAs are i.i.d Gaussian random variables

$$\delta_{n,AoA} \sim \eta(0, \sigma_{n,AoA}^2), \quad n = 1, \dots, N,$$

where  $\sigma_{n,AoA} = 104.12 \left( 1 - \exp(-0.265 |10 \log_{10}(P_n)|) \right)$  and  $P_n$  is the relative power of the  $n$ th path from Step 5.

When the LOS model is used, the AoA for the direct component is set equal to the line-of-sight path direction.

**Step 11:** Determine the offset AoAs of the  $M = 20$  sub-paths for each of the  $N$  paths at the MS.

**Step 12:** Associate the BS and MS paths and sub-paths. Sub-paths are randomly paired for each path, and the sub-path phases defined at the BS and MS are maintained.

**Step 13:** Determine the antenna gains of the BS and MS sub-paths as a function of their respective sub-path AoDs and AoAs.

**Step 14:** Apply the path loss based on the BS to MS distance and the log normal shadow fading determined in Step 3 as bulk parameters to each of the sub-path powers of the channel model.

**Table 5.2: Sub-path AoD and AoA offsets**

| Sub-path #<br>( <i>m</i> ) | Offset for a 2 deg AS at<br>BS (Macrocell)<br>$\Delta_{n,m,AoD}$ (degrees) | Offset for a 5 deg AS at<br>BS (Microcell)<br>$\Delta_{n,m,AoD}$ (degrees) | Offset for a 35 deg AS<br>at MS<br>$\Delta_{n,m,AoA}$ (degrees) |
|----------------------------|--|--|---|
| 1, 2                       | $\pm 0.0894$   | $\pm 0.2236$   | $\pm 1.5649$  |
| 3, 4                       | $\pm 0.2826$   | $\pm 0.7064$   | $\pm 4.9447$  |
| 5, 6                       | $\pm 0.4984$   | $\pm 1.2461$   | $\pm 8.7224$  |
| 7, 8                       | $\pm 0.7431$   | $\pm 1.8578$   | $\pm 13.0045$   |
| 9, 10                      | $\pm 1.0257$   | $\pm 2.5642$   | $\pm 17.9492$   |
| 11, 12                     | $\pm 1.3594$   | $\pm 3.3986$   | $\pm 23.7899$   |
| 13, 14                     | $\pm 1.7688$   | $\pm 4.4220$   | $\pm 30.9538$   |
| 15, 16                     | $\pm 2.2961$   | $\pm 5.7403$   | $\pm 40.1824$   |
| 17, 18                     | $\pm 3.0389$   | $\pm 7.5974$   | $\pm 53.1816$   |
| 19, 20                     | $\pm 4.3101$   | $\pm 10.7753$  | $\pm 75.4274$   |
|                            |  |  |   |

The values in Table 5.2 are selected to produce a biased standard deviation equal to 2, 5, and 35 degrees, which is equivalent to the per-path power weighted azimuth spread for equal power sub-paths.

## 5.4 Generating channel coefficients

Given the user parameters generated in Clause 5.3, we use them to generate the channel coefficients. For an  $S$  element linear BS array and a  $U$  element linear MS array, the channel coefficients for one of  $N$  multipath components are given by a  $U$ -by- $S$  matrix of complex amplitudes. We denote the channel matrix for the  $n$ th multipath component ( $n = 1, \dots, N$ ) as  $\mathbf{H}_n(t)$ . The  $(u, s)$ th component ( $s = 1, \dots, S$ ;  $u = 1, \dots, U$ ) of  $\mathbf{H}_n(t)$  is given by

$$h_{u,s,n}(t) = \sqrt{\frac{P_n \sigma_{SF}}{M}} \sum_{m=1}^M \left( \begin{array}{l} \sqrt{G_{BS}(\theta_{n,m,AoD})} \exp(j[kd_s \sin(\theta_{n,m,AoD}) + \Phi_{n,m}]) \times \\ \sqrt{G_{MS}(\theta_{n,m,AoA})} \exp(jkd_u \sin(\theta_{n,m,AoA})) \times \\ \exp(jk\|\mathbf{v}\| \cos(\theta_{n,m,AoA} - \theta_v)) \end{array} \right)$$

where

- $P_n$  is the power of the  $n$ th path (Step 5).
- $\sigma_{SF}$  is the lognormal shadow fading (Step 3), applied as a bulk parameter to the  $n$  paths for a given drop.
- $M$  is the number of subpaths per-path.
- $\theta_{n,m,AoD}$  is the the AoD for the  $m$ th subpath of the  $n$ th path (Step 12).
- $\theta_{n,m,AoA}$  is the the AoA for the  $m$ th subpath of the  $n$ th path (Step 12).
- $G_{BS}(\theta_{n,m,AoD})$  is the BS antenna gain of each array element (Step 12).
- $G_{MS}(\theta_{n,m,AoA})$  is the MS antenna gain of each array element (Step 12).
- $j$  is the square root of -1.
- $k$  is the wave number  $2\pi/\lambda$  where  $\lambda$  is the carrier wavelength in meters.
- $d_s$  is the distance in meters from BS antenna element  $s$  from the reference ( $s = 1$ ) antenna. For the reference antenna  $s = 1$ ,  $d_1 = 0$ .

|                  |   |
|------------------|---|
| $d_u$            | is the distance in meters from MS antenna element $u$ from the reference ( $u = 1$ ) antenna. For the reference antenna $u = 1$ , $d_1 = 0$ . |
| $\Phi_{n,m}$     | is the phase of the $m$ th subpath of the $n$ th path (Step 8).   |
| $\ \mathbf{v}\ $ | is the magnitude of the MS velocity vector (Step 2).  |
| $\theta_v$       | is the angle of the MS velocity vector (Step 2).  |

The path loss and the log normal shadowing is applied as bulk parameters to each of the sub-path components of the  $n$  path components of the channel.

## 5.5 Optional system simulation features

### 5.5.1 Polarized arrays

Practical antennas on handheld devices require spacings much less than  $\lambda/2$ . Polarized antennas are likely to be the primary way to implement multiple antennas. A cross-polarized model is therefore included here.

A method of describing polarized antennas is presented, which is compatible with the 13 step procedure given in Clause 5.3. The following steps replace step 13 with the new steps 13-19 to account for the additional polarized components. The ( $S/2$ )-element BS arrays and ( $U/2$ )-element MS arrays consist of  $U$  and  $S$  (i.e., twice in number) antennas in the V, H, or off-axis polarization.

**Step 13:** *Generate additional cross-polarized subpaths.* For each of the 6 paths of Step 4, generate an additional  $M$  subpaths at the MS and  $M$  subpaths at the BS to represent the portion of each signal that leaks into the cross-polarized antenna orientation due to scattering.

**Step 14:** *Set subpath AoDs and AoAs.* Set the AoD and AoA of each subpath in Step 13 equal to that of the corresponding subpath of the co-polarized antenna orientation. (Orthogonal sub-rays arrive/depart at common angles.)

**Step 15:** *Generate phase offsets for the cross-polarized elements.* We define  $\Phi_{n,m}^{(x,y)}$  to be the phase offset of the  $m$ th subpath of the  $n$ th path between the  $x$  component (e.g. either the horizontal  $h$  or vertical  $v$ ) of the BS element and the  $y$  component (e.g. either the horizontal  $h$  or vertical  $v$ ) of the MS element. Set  $\Phi_{n,m}^{(x,x)}$  to be  $\Phi_{n,m}$  generated in Step 8 of Clause 5.3. Generate  $\Phi_{n,m}^{(x,y)}$ ,  $\Phi_{n,m}^{(y,x)}$ , and  $\Phi_{n,m}^{(y,y)}$  as i.i.d random variables drawn from a uniform 0 to 360 degree distribution. ( $x$  and  $y$  can alternatively represent the co-polarized and cross-polarized orientations.)

**Step 16:** Decompose each of the co-polarized and cross-polarized sub-rays into vertical and horizontal components based on the co-polarized and cross-polarized orientations.

**Step 17:** The coupled power  $P_2$  of each sub-path in the horizontal orientation is set relative to the power  $P_1$  of each sub-path in the vertical orientation according to an XPD ratio, defined as  $XPD = P_1/P_2$ . A single XPD ratio applies to all sub-paths of a given path. Each path  $n$  experiences an independent realization of the XPD. For each path the realization of the XPD is drawn from the distributions below.

For urban macrocells:  $P_2 = P_1 - A - B * \eta(0,1)$ , where  $A = 0.34 * (\text{mean relative path power in dB}) + 7.2$  dB, and  $B = 5.5$  dB is the standard deviation of the XPD variation.

For urban microcells:  $P_2 = P_1 - A - B * \eta(0,1)$ , where  $A = 8$  dB, and  $B = 8$  dB is the standard deviation of the XPD variation.

The value  $\eta(0,1)$  is a zero mean Gaussian random number with unit variance and is held constant for all sub-paths of a given path.

By symmetry, the coupled power of the opposite process (horizontal to vertical) is the same. The V-to-H XPD draws are independent of the H-to-V draws.

**Step 18:** At the receive antennas, decompose each of the vertical and horizontal components into components that are co-polarized with the receive antennas and sum the components. This procedure is performed within the channel coefficient expression given below.

**Step 19:** Apply the path loss based on the BS to MS distance from Step 2, and the log normal shadow fading determined in step 3 as bulk parameters to each of the sub-path powers of the channel model.

The fading behavior between the cross pol elements will be a function of the per-ray spreads and the Doppler. The fading between orthogonal polarizations has been observed to be independent and therefore the sub-rays phases are chosen randomly. The propagation characteristics of V-to-V paths are assumed to be equivalent to the propagation characteristics of H-to-H paths.

The polarization model can be illustrated by a matrix describing the propagation of and mixing between horizontal and vertical amplitude of each sub-path. The resulting channel realization is:

$$h_{u,s,n}(t) = \sqrt{\frac{P_n \sigma_{SF}}{M}} \sum_{m=1}^M \left( \begin{bmatrix} \chi_{BS}^{(v)}(\theta_{n,m,AoD}) \\ \chi_{BS}^{(h)}(\theta_{n,m,AoD}) \end{bmatrix}^T \begin{bmatrix} \exp(j\Phi_{n,m}^{(v,v)}) & \sqrt{r_{n1}} \exp(j\Phi_{n,m}^{(v,h)}) \\ \sqrt{r_{n2}} \exp(j\Phi_{n,m}^{(h,v)}) & \exp(j\Phi_{n,m}^{(h,h)}) \end{bmatrix} \begin{bmatrix} \chi_{MS}^{(v)}(\theta_{n,m,AoA}) \\ \chi_{MS}^{(h)}(\theta_{n,m,AoA}) \end{bmatrix} \times \exp(jkd_s \sin(\theta_{n,m,AoD})) \times \exp(jkd_u \sin(\theta_{n,m,AoA})) \times \exp(jk\|\mathbf{v}\| \cos(\theta_{n,m,AoA} - \theta_v) t) \right)$$

where:

$\chi_{BS}^{(v)}(\theta_{n,m,AoD})$  is the BS antenna complex response for the V-pol component.

$\chi_{BS}^{(h)}(\theta_{n,m,AoD})$  is the BS antenna complex response for the H-pol component.

$\chi_{MS}^{(v)}(\theta_{n,m,AoA})$  is the MS antenna complex response for the V-pol component.

$\chi_{MS}^{(h)}(\theta_{n,m,AoA})$  is the MS antenna complex response for the H-pol component.

$|\chi^{(\cdot)}(\cdot)|^2$  is the antenna gain

$r_{n1}$  is the random variable representing the power ratio of waves of the nth path leaving the BS in the vertical direction and arriving at the MS in the horizontal direction (v-h) to those leaving in the vertical direction and arriving in the vertical direction (v-v).

$r_{n2}$  is the random variable representing the power ratio of waves of the nth path leaving the BS in the horizontal direction and arriving at the MS in the vertical direction (h-v) to those leaving in the vertical direction and arriving in the vertical direction (v-v). The variables  $r_{n1}$  and  $r_{n2}$  are i.i.d.

$\Phi_{n,m}^{(x,y)}$  phase offset of the mth subpath of the nth path between the x component (either the horizontal h or vertical v) of the BS element and the y component (either the horizontal h or vertical v) of the MS element.

The other variables are described in Clause 5.4. Note that the description above corresponds to a transmission from the base to mobile. The appropriate subscript and superscript changes should be made for uplink transmissions.

The 2x2 matrix represents the scattering phases and amplitudes of a plane wave leaving the UE with a given angle and polarization and arriving Node B with another direction and polarization.  $r_{\text{avg}}$  is the average power ratio of waves leaving the UE in the vertical direction and arriving at Node B in the horizontal direction (v-h) to those arriving at Node B in the vertical direction (v-v). By symmetry the power ratio of the opposite process (h-v over v-v) is chosen to be the same. Note that:  $r_{\text{avg}} = 1/\text{XPD}$ ; for the macrocell model, the XPD is dependent on the path index; for the microcell model, the XPD is independent of path index.

Expression (2) assumes a random pairing of the of the sub-paths from the MS and BS. The random orientation of the MS (UE) array affects the value of the angle  $\theta_{n,m,AoA}$  of each sub-path.



If for example, only vertically polarized antennas are used at both NodeB and UE then the antenna responses become

$\begin{bmatrix} 1 \\ 0 \end{bmatrix}$  and expression (2) becomes identical to (1). For an ideal dipole antenna at the NodeB tilted with respect to the z-axis at  $\alpha$  degrees the above vector becomes  $\begin{bmatrix} \cos(\alpha) \\ \sin(\alpha) \cdot \cos(\theta_{n,m,AoA}) \end{bmatrix}$ .

The elevation spectrum is not modeled.

## 5.5.2 Far scatterer clusters

The Far scatterer cluster model is switch selectable. It represents the bad-urban case where additional clusters are seen in the environment. This model is limited to use with the urban macro-cell where the first cluster will be the primary cluster and the second will be the far scattering cluster (FSC). When the model is active, it will have the following characteristics:

There is a reduction in the number of paths in the primary cluster from  $N = 6$  to  $N_1 = 4$ , with the far scattering cluster then having  $N_2 = 2$ . Thus the total number of paths will stay the same, now  $N = N_1 + N_2 = 4 + 2$ . This is a modification to the SCM channel generation procedure in Clause 5.3.

The FSCs will only be modeled for the serving cell, with 3 independent FSCs in the cell uniformly applied to the area of the cell outside the minimum radius.

The following is a generation procedure for the FSC model and is used in conjunction with the normal channel generation procedure in Clause 5.3.

**Step 1.** Drop the MS within test cell.

**Step 2.** Drop three FS clusters uniformly across the cell hexagon, with a minimum radius of  $R = 500\text{m}$ .

**Step 3.** Choose the FS cluster to use for the mobile that is closest to the mobile.

**Step 4.** Generate 6 delays  $\tau_1, \tau_2, \tau_3, \tau_4, \tau_5, \tau_6$ .

**Step 5.** Sort  $\tau_1, \tau_2, \tau_3, \tau_4$  in order of increasing delays,

**Step 6.** Subtract shortest delay of  $\tau_1, \tau_2, \tau_3, \tau_4$  from each of  $\tau_1, \tau_2, \tau_3, \tau_4$ .

**Step 7.** Sort  $\tau_5, \tau_6$  in the order of increasing delays,

**Step 8.** Subtract shorter delay of  $\tau_5, \tau_6$  from each of  $\tau_5, \tau_6$ .

**Step 9.** Assign powers to paths corresponding to all 6 delays:

$$P'_n = e^{\frac{(1-r_{DS})\tau'_n}{r_{DS} \cdot \sigma_{DS}}} \cdot 10^{-\xi_n/10}, n = 1, \dots, 6$$

where  $\xi_n$  ( $n = 1, \dots, 6$ ) are i.i.d. Gaussian random variables with standard deviation  $\sigma_{RND} = 3$  dB.

**Step 10.** Calculate excess path delay  $\tau_{excess}$  and add to  $\tau_5, \tau_6$ .

**Step 11.** Attenuate P5 and P6 by  $1\text{dB}/\mu\text{s}$  of excess delay with a  $10\text{dB}$  maximum attenuation. The excess delay will be defined as the difference in propagation time between the BS-MS LOS distance, and the BS-FSC-MS distance.

**Step 12.** Scale each of the powers in the main cluster and in the FSC by a common log normal randomizing factor of  $8\text{dB}/\sqrt{2}$  drawn once per cluster to represent the effect of the independent per cluster shadow fading after including site correlation of the mobile location.

**Step 13.** Normalize powers of the 6 paths to unity power.

**Step 14.** Select AoDs at the BS for the main cluster from the channel generation procedure in Clause 5.3. Select AoDs at the BS for the FSC referenced to the direction of the FSC and selecting values from a Gaussian distribution with

standard deviation  $r_{AS} \cdot \text{mean}(AS)$ , where the  $\text{mean}(AS)$  is equal to 8 degrees or 15 degrees, chosen to match the angle spread model used.

**Step 15.** Select AoAs at the MS using the equation in step 9 of Clause 5.3, where the 4 paths associated with the main cluster are referenced to the LOS direction to the BS, and the 2 paths associated with the FSC are referenced to the direction of the FSC. The relative powers used are the normalized powers of step 13 of this clause.

**Step 16.** Apply the bulk path loss and log normal to all 6 paths and apply the antenna gains accounting for the angles of the sub-paths associated with the main cluster and the FSC.

### 5.5.3 Line of sight

The line-of-sight (LOS) model is an option that is switch selectable for the urban micro scenario only. LOS modelling will not be defined for the suburban or urban macro cases due to the low probability of occurrence. The LOS modelling is based on the Ricean K factor defined as the ratio of power in the LOS component to the total power in the diffused non line-of-sight (NLOS) component. The K factor may be defined in dB or linear units in the equations in this document. The LOS component is a direct component and therefore has no per-path angle spreading. The LOS model uses the following description when this function is selected.

For the NLOS case, the Ricean K factor is set to 0, thus the fading is determined by the combination of sub-rays as described in Clause 5.3 of the model.

For the LOS case, the Ricean K factor is based on a simplified version of [1] :  $K = 13 - 0.03 \cdot d$  (dB) where d is the distance between MS and BS in meters.

The probability for LOS or NLOS depends on various environmental factors, including clutter, street canyons, and distance. For simplicity, the probability of LOS is defined to be unity at zero distance, and decreases linearly until a cutoff point at  $d=300\text{m}$ , where the LOS probability is zero.

$$P(LOS) = \begin{cases} (300 - d) / 300, & 0 < d < 300\text{m} \\ 0, & d > 300\text{m} \end{cases}$$

The K-factor, propagation slope, and shadow fading standard deviation will all be chosen based on the results of selecting the path to be LOS or NLOS.

The total combined power of the LOS component and the 6 diffuse components is normalized to unity power so the

coherent LOS component will have a relative amplitude  $\sqrt{\frac{K}{K+1}}$  and the amplitudes of all 6 diffuse paths will have a

relative amplitude  $\sqrt{\frac{1}{K+1}}$ , where K is in linear units. The LOS path will coincide in time (but not necessarily in angle)

with the first (earliest) diffused path. When pairing sub-rays between transmitter and receiver, the direct components are paired representing the LOS path. The AoD and AoA of the LOS component are given by  $\theta_{BS}$  and  $\theta_{MS}$ , respectively.

Following the definitions in Clause 5.4, the  $(u,s)$ th component of the channel coefficient ( $s = 1, \dots, S$ ;  $u = 1, \dots, U$ ) and path n is given by:

$$h_{s,u,n=1}^{LOS}(t) = \sqrt{\frac{1}{K+1}} h_{s,u,1}(t) + \sigma_{SF} \sqrt{\frac{K}{K+1}} \left( \begin{aligned} & \sqrt{G_{BS}(\theta_{BS})} \exp(jkd_s \sin(\theta_{BS})) \times \\ & \sqrt{G_{MS}(\theta_{MS})} \exp(jkd_u \sin(\theta_{MS}) + \Phi_{LOS}) \times \\ & \exp(jk\|v\| \cos(\theta_{MS} - \theta_v) t) \end{aligned} \right)$$

$$\text{and for } n \neq 1: h_{s,u,n}^{LOS}(t) = \sqrt{\frac{1}{K+1}} h_{s,u,n}(t)$$

where  $h_{s,u,n}(t)$ ;  $n=1, \dots, N$  is as defined in Clause 5.4 and:

|                |  |
|----------------|--|
| $\theta_{BS}$  | is the the AoD for the LOS component at the base     |
| $\theta_{MS}$  | is the the AoA for the LOS component at the terminal |
| $\theta_{LOS}$ | is the phase of the LOS component                    |

$K$  is the K factor

### 5.5.4 Urban canyon

The urban canyon model is switch selectable. When switched on, the model modifies the AoAs of the paths arriving at the subscriber unit. It is for use in both the urban macro and urban micro scenarios.

Urban-canyons exist in dense urban areas served by macro-cells, and for at-rooftop micro-cells. When this model is used, the spatial channel for all subscribers in the simulated universe will be defined by the statistical model given below. Thus for the SCM channel generation steps given in Clause 5.3, Step 9 is replaced with steps 9a-d given below, which describe the AoAs of the paths arriving at the subscriber in the urban canyon scenario.

The following procedure is used to determine the subscriber mean AoAs of the six paths. This model does not use a building grid, but assigns angles based on statistical data presented in the figures below. The procedure is defined in terms of the subscriber terminal:

**Step 9a.** Select a random street orientation from:  $U(0, 360^\circ)$  which also equals the direction of travel for the UE.

**Step 9b.** Select a random orientation for the subscriber antenna array from  $U(0, 360)$ .

**Step 9c.** Given  $\alpha = 0.9$  the predefined fraction of UEs to experience the urban canyon effect, Select a uniform random draw for the parameter  $\beta$ .

**Step 9d.** If  $\beta \leq \alpha$ , select the UE AoAs for all arriving paths to be equal, with 50% probability of being from the direction of the street orientation obtained in step 9a, and 50% the street orientation plus an offset of  $180^\circ$ . If  $\beta > \alpha$  select the directions of arrival for all paths using the standard SCM UE AoA model given in Clause 5.3, step 9.

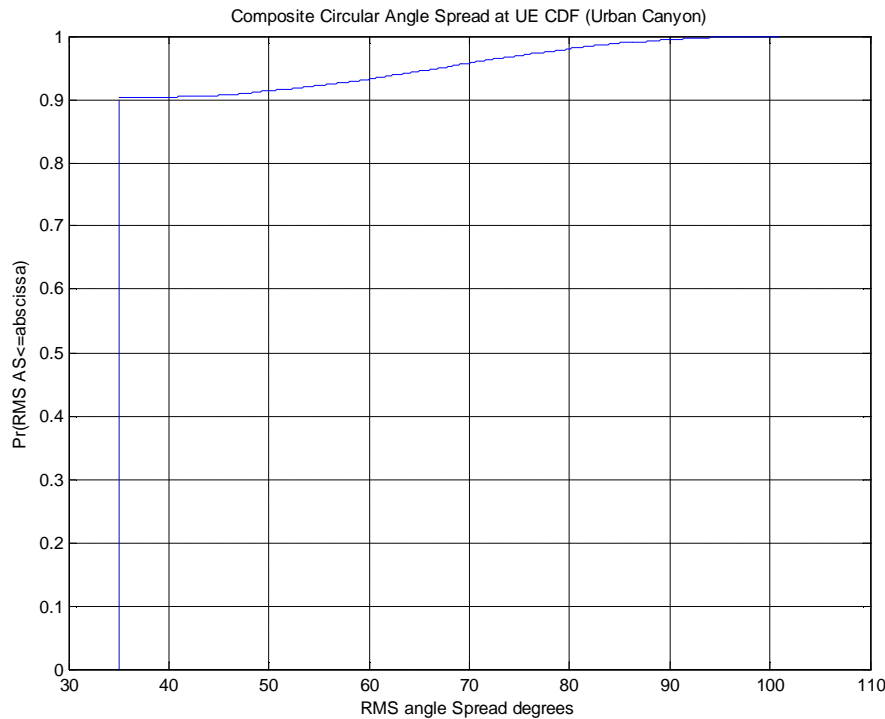


**Figure 5.3. Simulated results of urban canyon algorithm for  $\alpha = 0.9$**

In Figure 5.3, the urban canyon procedure is simulated to show the effects of the model on the composite UE angle spread. The parameter  $\alpha = 0.9$ , which describes the percentage of mobiles that will experience the urban canyon effects. The figure illustrates the result of selecting the AoAs, where each of the paths has a fixed  $35^\circ$  angle spread.

The parameter  $\alpha = 0.9$ , is set to a relatively high percentage of occurrence to emphasize the urban canyon effects, while the remaining occurrences assume some mixed arrivals to model various other conditions such as cross streets or where signals arrive from between buildings or from unknown paths at various angles.

## 5.6 Correlation between channel parameters

In [2], Greenstein presents a model for correlating delay spread (DS) with log normal shadow fading (SF). Since both are shown to be log-normal distributed, DS and SF are generally correlated.

The result of the negative correlation between log normal shadowing and delay spread is significant because it indicates that for a larger SF, the DS is reduced, and for a smaller SF, the DS is increased.

Cost 259[3] presents the azimuth spread (AS) as also being log-normal distributed, and likewise being correlated to the DS and SF. Since the correlation of these parameters is quite high, a spatial channel model needs to be specified that can reproduce this correlation behavior along with the expected probability and range of each parameter. To make sure the model is self-consistent and the full correlation matrix is positive semi-definite, the intra-site correlations between SF, DS and AS are as follows:

$$\rho_{\alpha\beta} = \text{Correlation between DS \& AS} = +0.5$$

$$\rho_{\gamma\beta} = \text{Correlation between SF \& AS} = -0.6$$

$$\rho_{\gamma\alpha} = \text{Correlation between SF \& DS} = -0.6$$

The resulting intra-site correlation matrix is given by **A**:

$$\mathbf{A} = \begin{bmatrix} 1 & \rho_{\alpha\beta} & \rho_{\gamma\alpha} \\ \rho_{\alpha\beta} & 1 & \rho_{\gamma\beta} \\ \rho_{\gamma\alpha} & \rho_{\gamma\beta} & 1 \end{bmatrix}$$

In addition to intra-site correlations given by **A**, there are also correlations between of these parameters between different sites. These inter-site correlations are given by

$$\mathbf{B} = \begin{bmatrix} 0 & 0 & 0 \\ 0 & 0 & 0 \\ 0 & 0 & \zeta \end{bmatrix}$$

Essentially, only inter-site correlations between SF are included.  $\zeta$  is the SF correlation which is = 0.5.

Suppose we wish to generate the values for DS, AS, and SF for the  $n$ th base station ( $n = 1 \dots N$ ) with respect to a given mobile user. These values are given as  $\sigma_{DS,n}$ ,  $\sigma_{AS,n}$ , and  $\sigma_{SF,n}$ , respectively. These values are a function of the respective correlated Gaussian random variables  $\alpha_n$ ,  $\beta_n$ , and  $\gamma_n$ . These correlated Gaussian random variables are in turn respectively generated from independent Gaussian random variables  $w_{n1}$ ,  $w_{n2}$ , and  $w_{n3}$  as well as three global (applicable to all bases) independent Gaussian random variables  $\xi_1, \xi_2, \xi_3$ . The variables  $\alpha_n$ ,  $\beta_n$ , and  $\gamma_n$  are then given by:

$$\begin{bmatrix} \alpha_n \\ \beta_n \\ \gamma_n \end{bmatrix} = \begin{bmatrix} c_{11} & c_{12} & c_{13} \\ c_{21} & c_{22} & c_{23} \\ c_{31} & c_{32} & c_{33} \end{bmatrix} \begin{bmatrix} w_{n1} \\ w_{n2} \\ w_{n3} \end{bmatrix} + \begin{bmatrix} 0 & 0 & 0 \\ 0 & 0 & 0 \\ 0 & 0 & \sqrt{\zeta} \end{bmatrix} \begin{bmatrix} \xi_1 \\ \xi_2 \\ \xi_3 \end{bmatrix}$$

where the matrix **C** with elements  $c_{ij}$  multiplying the  $w$ 's is given by

$$\mathbf{C} = (\mathbf{A} - \mathbf{B})^{1/2} = \begin{bmatrix} 1 & \rho_{\alpha\beta} & \rho_{\gamma\alpha} \\ \rho_{\alpha\beta} & 1 & \rho_{\gamma\beta} \\ \rho_{\gamma\alpha} & \rho_{\gamma\beta} & 1 - \zeta \end{bmatrix}^{1/2}$$

where the superscript “ $\frac{1}{2}$ ” denotes the matrix square root. The distribution of DS for the  $n$ th BS is given by:

$$\sigma_{DS,n} = 10^{\frac{1}{2}(\varepsilon_{DS}\alpha_n + \mu_{DS})}$$

where  $\alpha_n$  is generated above,  $\mu_{DS} = E(\log_{10}(\sigma_{DS}))$  is the logarithmic mean of the distribution of DS, and  $\varepsilon_{DS} = \sqrt{E[\log_{10}^2(\sigma_{DS,n})] - \mu_{DS}^2}$  is the logarithmic standard deviation of the distribution of DS.

Similarly the distribution of AS is given by:

$$\sigma_{AS,n} = 10^{\frac{1}{2}(\varepsilon_{AS}\beta_n + \mu_{AS})}$$

where  $\beta_n$  is generated above,  $\mu_{AS} = E(\log_{10}(\sigma_{AS}))$  is the logarithmic mean of the distribution of AS, and  $\varepsilon_{AS} = \sqrt{E[\log_{10}^2(\sigma_{AS,n})] - \mu_{AS}^2}$  is the logarithmic standard deviation of the distribution of AS.

Finally, the distribution for SF is given by:

$$\sigma_{SF,n} = 10^{\frac{1}{2}(\sigma_{SH}\gamma_n/10)}$$

where  $\gamma_n$  is given above, and  $\sigma_{SH}$  is the shadow fading standard deviation given in dB. The value of  $\sigma_{SH}$  is obtained from analysis of the standard deviation from the regression line of the path loss versus distance. As shown in Table 5.1, these values are 8dB and 10dB for the macro and microcell cases, respectively. Note that the dB value for SF is simply  $\sigma_{SH}\gamma_n$ .

## 5.7 Modeling intercell interference

Sophisticated MIMO receivers account for the spatial characteristics of the signals from the desired sector as well as from the interfering sectors. The spatial characteristics of these signals can be modeled according to the channel matrix generated according to Clauses 5.3, 5.4, and 5.5. However, it may be prohibitively complex to explicitly model the spatial characteristics of all interfering sectors, especially those whose received powers are relatively weak. It has been shown that by modelling the signals of relatively weak interferers as spatially white (and thereby ignoring their spatial characteristics), the resulting performance difference is negligible. The following four steps outline the procedure for modelling intercell interference.

- Determine the pathloss and shadowing of all sectors. (Note that "pathloss" implicitly includes antenna patterns as well.)
- Rank the sectors in order of received power (based on pathloss and shadowing). The base with the strongest received power is the serving base, and the others are interfering bases.
- Model the strongest  $B$  interfering sectors as spatially correlated processes whose covariances are determined by their channel matrices. These channel matrices are generated from Clauses 5.3, 5.4, and 5.5 and account for the pathloss, shadowing, and fast fading variations. The way in which the channel realizations are employed depends on the receiver algorithm and simulation methodology. For example, if only the statistics of the interfering sectors are required, their signals can be modeled as spatially correlated additive Gaussian noise processes with covariances determined by the channel matrices.
- Model the remaining sectors as spatially white Gaussian noise processes whose variances are based on a flat Rayleigh fading process. Hence the variances are varying over the duration of a simulation drop.

To model the remaining "weak" sectors, we assume that the mean power of the flat Rayleigh fading process is equal to the effects of pathloss and shadowing from each sector. Therefore if the received power from the  $b$ -th sector due to pathloss and shadowing is  $\mathcal{P}_b$ , then the Rayleigh fading process for the  $m$ -th receive antenna ( $m = 1, \dots, M$ ) as a function of time is given by  $r_{b,m}(t)$  where the mean of  $r_{b,m}(t)$  over time is  $\mathcal{P}_b$ . The fading processes for each sector and receive antenna are independent, and the doppler rate is determined by the speed of the mobile. We assume that the fading is equivalent for each mobile receive antenna. The total received noise power per receive antenna due to all "weak" sectors at the  $m$ -th antenna is

$$\sum_{b \in F} r_{b,m}(t)$$

where  $F$  is the set of indices for the "weak" sectors.

For 3-sector systems, we model the  $B = 8$  strongest sectors. For 6-sector systems, we model  $B = 12$  strongest sectors. The values for  $B$  are based on simulation results for the typical cell layout with a single hexagonal cell surrounded by two rings of cells (a total of 19 cells) and with users placed in the center cell. For other layouts, different values of  $B$  or an entirely different technique may be required to properly account for the intercell interference.

## 5.8 System Level Calibration

The following examples are given for calibration purposes. A resolvable path at the receiver is assumed to be the energy from one (or more) paths falling within one chip interval. The Chip rate in UMTS is 3.84Mcps. The PDF of the number of resulting resolvable paths is recorded.

The following table is for interim calibration purposes. "Ideal" signifies the value taken from measurements, "Input" signifies the value used in generating a random variable, "Output" signifies the resulting measured statistic.

**Table 5.3: SCM parameter summary with simulated outputs**

| Parameter           | Suburban 5°<br>$\sigma_{\text{RND}} = 3\text{dB}$ |                     | Urban 8°<br>$\sigma_{\text{RND}} = 3\text{dB}$ |                    | Urban 15°<br>$\sigma_{\text{RND}} = 3\text{dB}$ |                    | Urban Micro<br>$\sigma_{\text{RND}} = 3\text{dB}$ |                     |
|---------------------|---|---------------------|--|--------------------|---|--------------------|---|---------------------|
| $r_{DS}$            | Input   | Output              | Input  | Output             |   | Output             |   |                     |
|                     | 1.4   | 1.29                | 1.7  | 1.54               | 1.7   | 1.54               |   |                     |
| $\mu_{DS}$          | Input   | Ideal               | Input  | Ideal              | Input   | Ideal              |   |                     |
|                     | -6.80   | -6.92               | -6.195   | -6.26              | -6.195  | -6.26              |   |                     |
| $\epsilon_{DS}$     | Input   | Ideal               | Input  | Ideal              | Input   | Ideal              |   |                     |
|                     | 0.288   | 0.363               | 0.18   | 0.25               | 0.18  | 0.25               |   |                     |
| $r_{AS}$            | Input   | Output              | Input  | Output             | Input   | Output             |   |                     |
|                     | 1.2   | 1.22                | 1.3  | 1.37               | 1.3   | 1.37               |   |                     |
| $\mu_{AS}$          | Input   | Ideal               | Input  | Ideal              | Input   | Ideal              |   |                     |
|                     | 0.69  | 0.66                | 0.810  | 0.75               | 1.18  | 1.0938             |   |                     |
| $\epsilon_{AS}$     | Input   | Ideal               | Input  | Ideal              | Input   | Ideal              |   |                     |
|                     | 0.13  | 0.18                | 0.34   | 0.37               | 0.21  | 0.2669             |   |                     |
| $E[\sigma_{DS}]$    | Ideal   | Output              | Ideal  | Output             | Ideal   | Output             |   | Output              |
|                     | 0.17 $\mu\text{s}$                                | 0.172 $\mu\text{s}$ | 0.65 $\mu\text{s}$                             | 0.63 $\mu\text{s}$ | 0.65 $\mu\text{s}$                              | 0.63 $\mu\text{s}$ |   | 0.251 $\mu\text{s}$ |
| $E[\sigma_{AS,BS}]$ | Ideal   | Output              | Ideal  | Output             | Ideal   | Output             | Ideal   | Output              |
|                     | 5°  | 5.01°               | 8°   | 7.97°              | 15°   | 14.9°              | 19°   | 19.2°               |
| $E[\sigma_{AS,MS}]$ | Ideal   | Output              | Ideal  | Output             | Ideal   | Output             | Ideal   | Output              |
|                     | 68°   | 69.2°               | 68°  | 68.3°              | 68°   | 68.04°             | 68°   | NLOS:<br>67.5°      |

The following figures: Figure 5.4, Figure 5.5, Figure 5.6, Figure 5.7, Figure 5.8, represent calibration cases for the current SCM model. Figure 5.9 illustrates the UE composite angle spread for a variety of SCM scenarios. These curves shown in the various figures correspond to the parameters presented in Table 5.3, and include the 3dB randomizing factor for the generation of path powers.

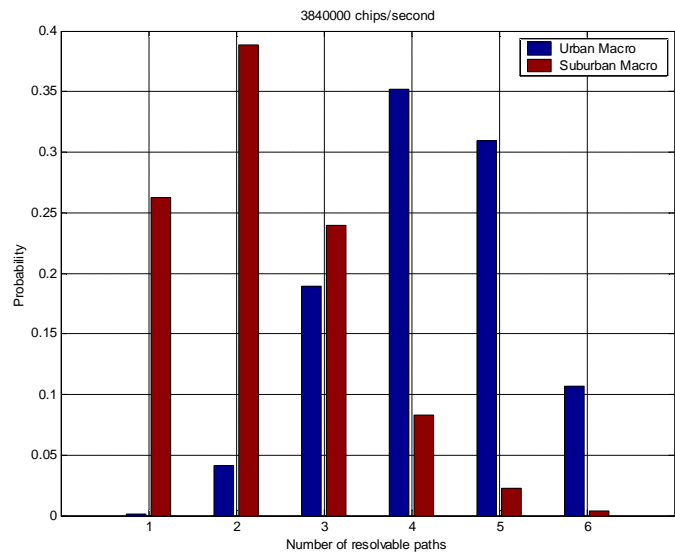


Figure 5.4: Probability of urban and suburban time resolvable paths

In this figure, powers are combined within a chip time as a simple way to estimate the number of resolvable paths.

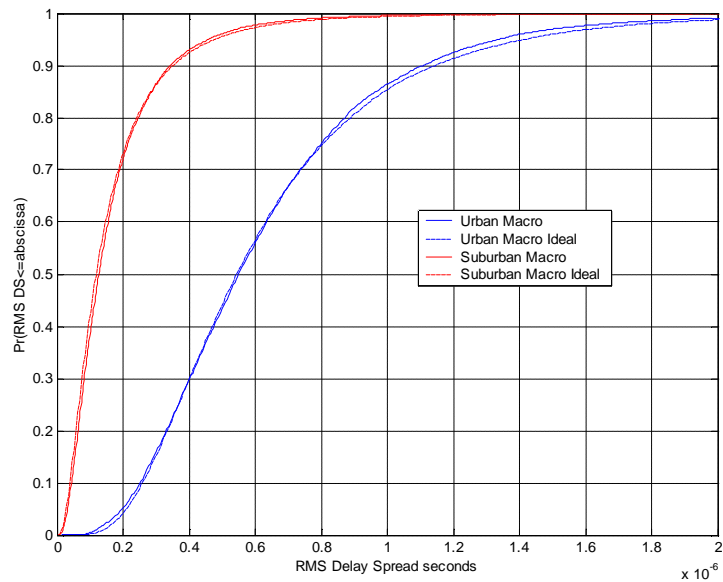
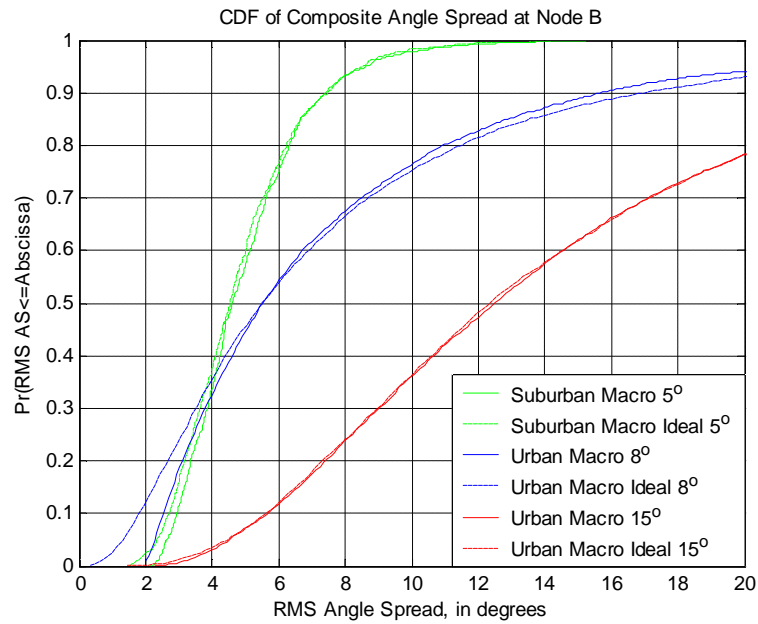
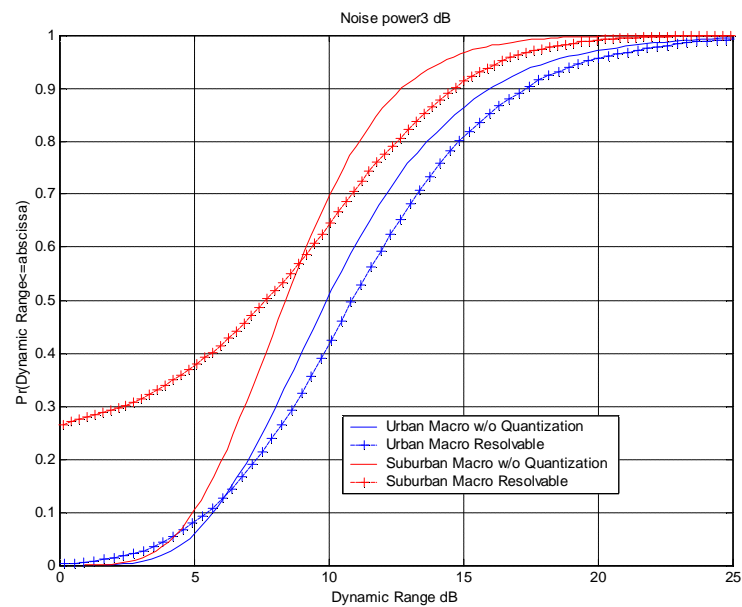


Figure 5.5: RMS delay spread, simulated versus ideal



**Figure 5.6: BS composite angle spread, simulated versus ideal**



**Figure 5.7: Dynamic range (dB) for each channel model**



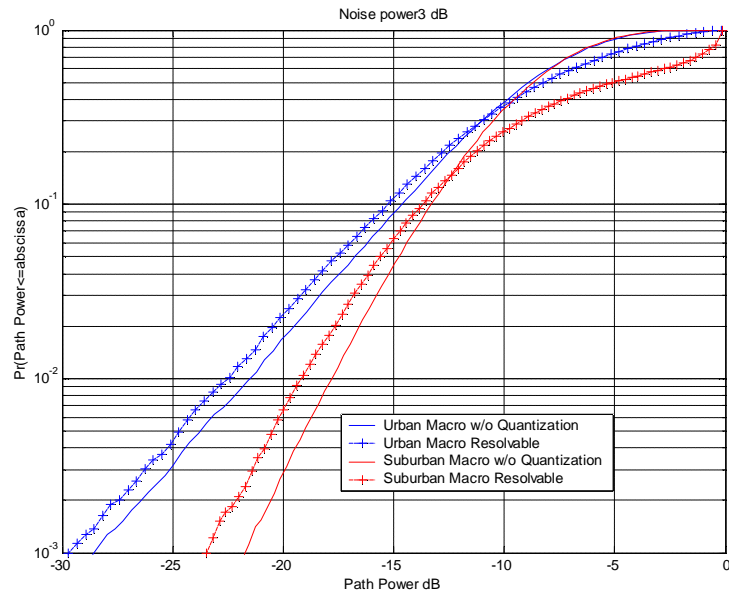


Figure 5.8: CDF of all path powers

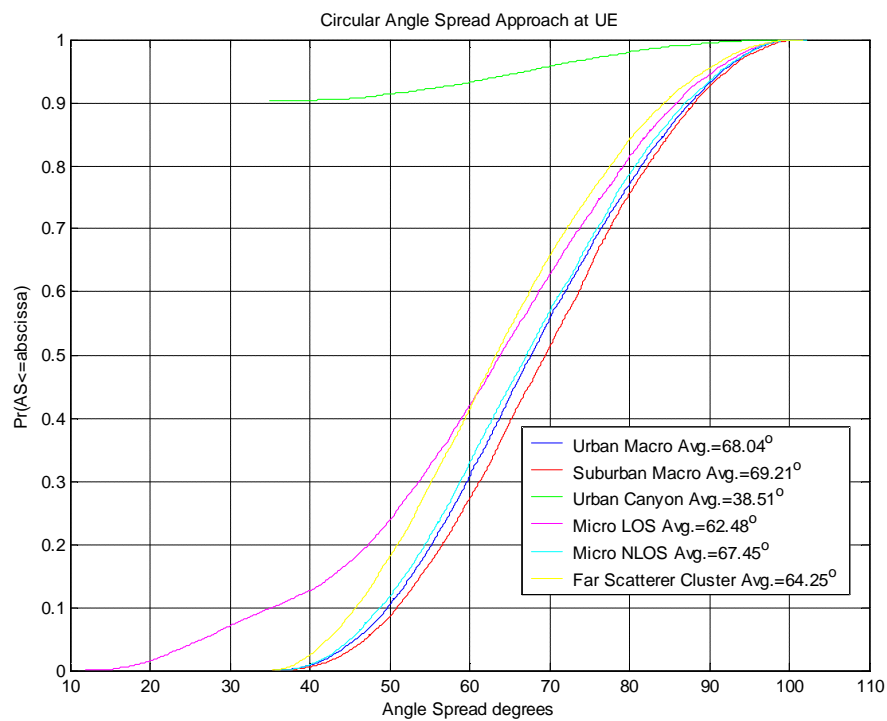


Figure 5.9: CDF of MS angle spread for various SCM scenarios (circular AS calculation)

## Channel Scenario: Urban Microcellular

A number of parameters are shown in the following plots which are the result of simulations. Figure 5.10 illustrates the dynamic range of each channel realization, plotted as a complementary cdf. The difference between the 1.25 MHz and 5 MHz channel bandwidths are shown in the resolvable dynamic range curves. (Powers are combined within a chip time as a simple way to estimate the resolvable powers.) The 1% highest value is approximately the same for both bandwidths. The dynamic range  $D$  is calculated from  $D = 10 \cdot \log_{10}(\max \text{ pwr} / \min \text{ pwr})$  for each channel realization.

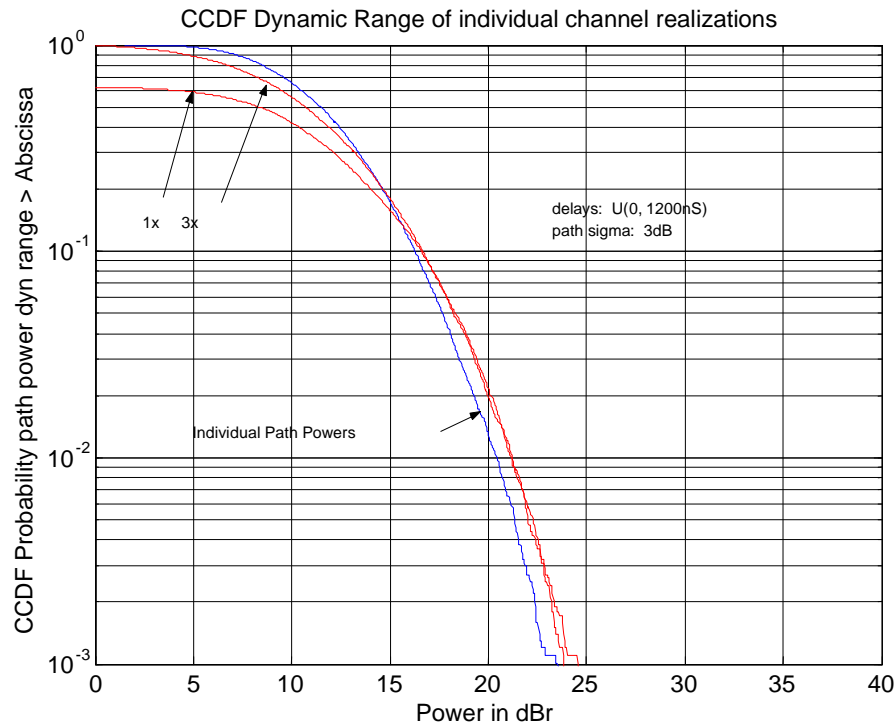


Figure 5.10: Dynamic range of path powers per channel realization, (NLOS)

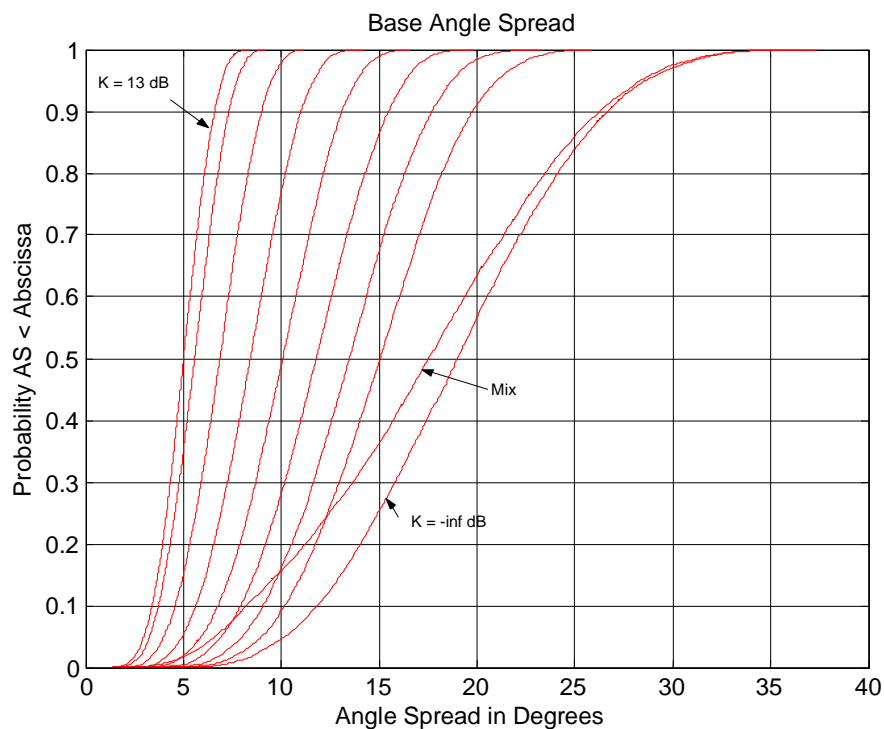
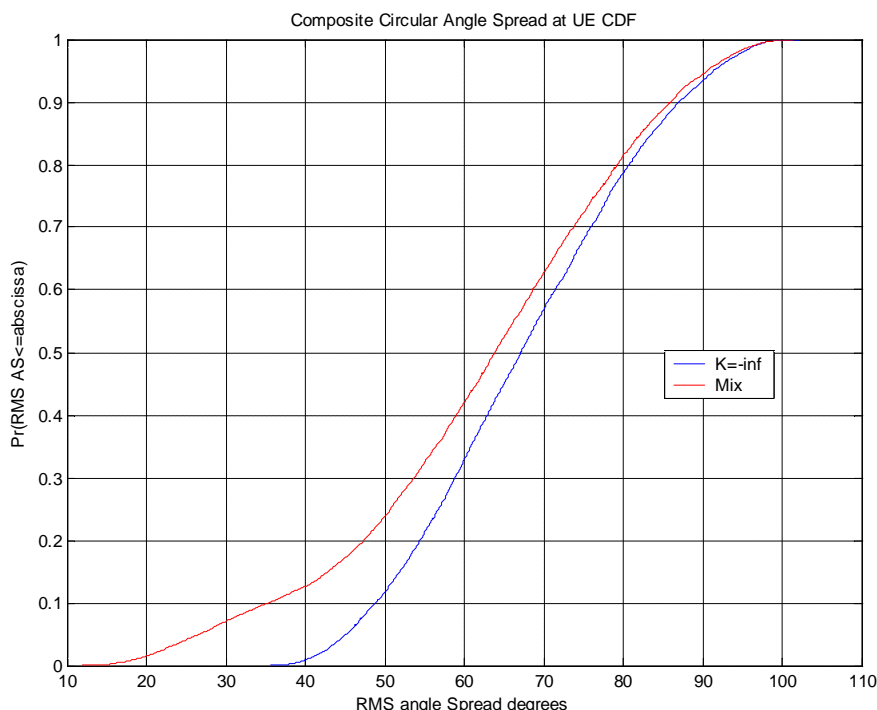


Figure 5.11: Composite BS angle spread

The composite angle spread at the base is described in Figure 5.11 for the various K-factors that are seen in the micro-cell model, along with the LOS/NLOS mix expected when the cell radius is 500m (as measured from the cell center to cell corner). For the NLOS case, the average composite Base AS = 19 degrees. When experiencing LOS paths with increased K-factors, the angle spreads are observed to decreased accordingly. The simulated average composite Base AS for the NLOS model is: 19.2 degrees, and the simulated average composite Base AS for the mixed propagation model is: 17.6 degrees.



**Figure 5.12: Composite MS angle spread**

The composite UE angle spread is described in Figure 5.12 for increased K-factor from a LOS path, causes the composite AS to be decreased since more power is present in a single direct component. The mixed case is shown which has a slight decrease in the statistics due to the 15% of the locations experiencing the LOS condition (assuming a cell radius of 500m). The simulated average composite UE AS for the NLOS model is: 67.45 degrees, and the simulated average composite UE AS for the mixed propagation model is: 62.48 degrees.

The delay spread is illustrated in Figure 5.13, which is also affected by the presence of a direct path. The mix is produced by the combination of LOS and NLOS paths. The simulated average delay spread for the NLOS condition is: 251 nS, and the simulated average delay spread for the mixed case is: 231 nS

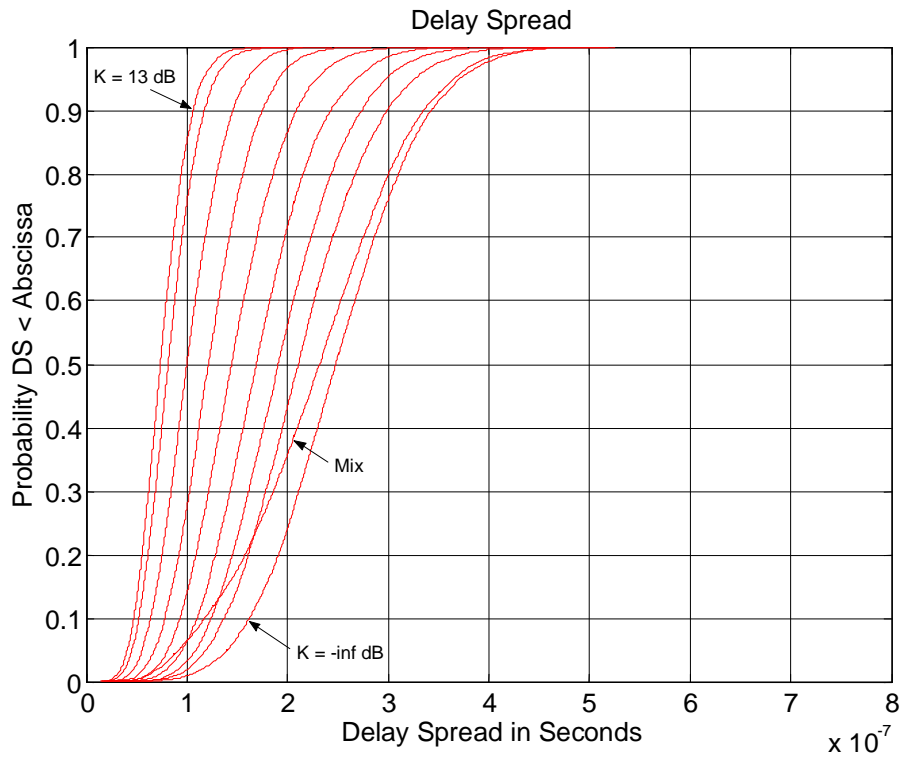


**Figure 5.13: Micro-cell delay spread**

Figure 5.14 illustrates the propagation path loss model of the urban microcell which is characterized by the mixed mode between LOS and NLOS.

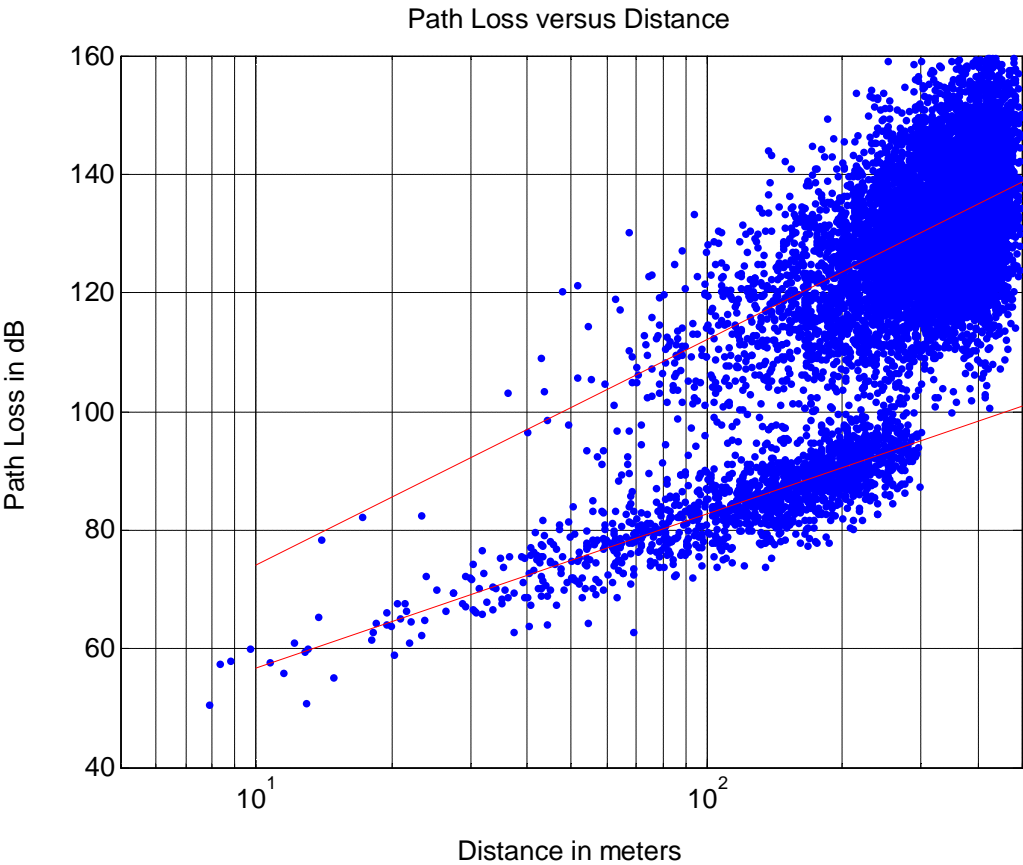


Figure 5.14: Microcell path loss versus distance

## Annex A: Calculation of circular angle spread

For a signal with  $N$  multi-paths, each has  $M$  sub-paths, the conventional angle spread calculation for the composite signal is given by

$$\sigma_{AS} = \sqrt{\frac{\sum_{n=1}^N \sum_{m=1}^M (\theta_{n,m,\mu})^2 \cdot P_{n,m}}{\sum_{n=1}^N \sum_{m=1}^M P_{n,m}}}$$

where  $P_{n,m} = P_n / 20$  is the power for the  $m$ th subpath of the  $n$ th path,  $\theta_{n,m,\mu}$  is defined as

$$\theta_{n,m,\mu} = \begin{cases} 2\pi + (\theta_{n,m} - \mu_\theta) & \text{if } (\theta_{n,m} - \mu_\theta) < -\pi \\ (\theta_{n,m} - \mu_\theta) & \text{if } |\theta_{n,m} - \mu_\theta| \leq \pi \\ 2\pi - (\theta_{n,m} - \mu_\theta) & \text{if } (\theta_{n,m} - \mu_\theta) > \pi \end{cases},$$

$\mu_\theta$  is defined as

$$\mu_\theta = \frac{\sum_{n=1}^N \sum_{m=1}^M \theta_{n,m} \cdot P_{n,m}}{\sum_{n=1}^N \sum_{m=1}^M P_{n,m}}$$

and  $\theta_{n,m}$  is the AoA (or AoD) of the  $m$ th subpath of the  $n$ th path. Note that we have dropped the AoA (AoD) subscript for convenience.

We note that the angle spread should be independent of a linear shift in the AoAs. In other words, by replacing  $\theta_{n,m}$  with  $\theta_{n,m} + \Delta$ , the angle spread  $\sigma_{AS}(\Delta)$  which is now a function of  $\Delta$  should actually be constant no matter what  $\Delta$  is. However, due to the ambiguity of the modulo  $2\pi$  operation, this may not be the case. Therefore the angle spread should be the minimum of  $\sigma_{AS}(\Delta)$  over all  $\Delta$ :

$$\sigma_{AS} = \min_{\Delta} \sigma_{AS}(\Delta) = \sqrt{\frac{\sum_{n=1}^N \sum_{m=1}^M (\theta_{n,m,\mu}(\Delta))^2 \cdot P_{n,m}}{\sum_{n=1}^N \sum_{m=1}^M P_{n,m}}}$$

where  $\theta_{n,m,\mu}(\Delta)$  is defined as

$$\theta_{n,m,\mu}(\Delta) = \begin{cases} 2\pi + (\theta_{n,m}(\Delta) - \mu_\theta(\Delta)) & \text{if } (\theta_{n,m}(\Delta) - \mu_\theta(\Delta)) < -\pi \\ (\theta_{n,m}(\Delta) - \mu_\theta(\Delta)) & \text{if } |\theta_{n,m}(\Delta) - \mu_\theta(\Delta)| \leq \pi \\ 2\pi - (\theta_{n,m}(\Delta) - \mu_\theta(\Delta)) & \text{if } (\theta_{n,m}(\Delta) - \mu_\theta(\Delta)) > \pi \end{cases},$$

$\mu_\theta(\Delta)$  is defined as

$$\mu_{\theta}(\Delta) = \frac{\sum_{n=1}^N \sum_{m=1}^M \theta_{n,m}(\Delta) \cdot P_{n,m}}{\sum_{n=1}^N \sum_{m=1}^M P_{n,m}}$$

and  $\theta_{n,m}(\Delta) = \theta_{n,m} + \Delta$ .

---

## Annex B: Change history

| Change history |        |           |     |     |  |       |       |
|----------------|--------|-----------|-----|-----|--|-------|-------|
| Date           | TSG #  | TSG Doc.  | CR  | Rev | Subject/Comment  | Old   | New   |
| 16/06/03       | RP_20  | RP-030311 | -   | -   | Approved as a Release 6 technical report                                 | 2.0.0 | 6.0.0 |
| 20/09/03       | RP_21  | RP-030461 | 001 | 2   | Corrections and clarifications to Spatial Channel Model Technical Report | 6.0.0 | 6.1.0 |
| 15/06/07       | SP_36  | -         | -   | -   | Update to Rel-7  | 6.1.0 | 7.0.0 |
| 05/12/08       | RAN_42 | -         | -   | -   | Update to Rel-8  | 7.0.0 | 8.0.0 |
| 07/12/09       | SP_46  | -         | -   | -   | Update to Rel-9  | 8.0.0 | 9.0.0 |
|                |        |           |     |     |  |       |       |
|                |        |           |     |     |  |       |       |
|                |        |           |     |     |  |       |       |